Maryland Department of Natural Resources
Resource Assessment Service
MARYLAND GEOLOGICAL SURVEY
Richard A. Ortt, Jr., Director

OPEN-FILE REPORT NO. 21-02-01

LAND SUBSIDENCE MONITORING TO ASSESS POTENTIAL EFFECTS OF GROUNDWATER WITHDRAWALS FROM COASTAL PLAIN AQUIFERS IN MARYLAND

FALL, 2020 SURVEY

by

Thomas Ulizio

Prepared in cooperation with the
Anne Arundel County Department of Public Works, Dominion Cove Point LNG/LP,
and the U.S. Geological Survey

DNR Publication No. 12-082021-286

2021

CONTENTS

ILLUSTRATIONS

ABBREVIATIONS USED IN THIS REPORT

General

4CID	four-character ID
COGO	coordinate geometry
CORS	continuously operating reference station
ESRI	Environmental Systems Research Institute
GIA	glacial isostatic adjustment
GNSS	Global Navigation Satellite System
GPS	global positioning system
IGS08	International GNSS Service 2008
ITRF14	International Terrestrial Reference Frame 2014
LNG	liquid natural gas
LP	limited partnership
MDE	Maryland Department of the Environment
MGS	Maryland Geological Survey
NAD83	North American Datum of 1983
NAVD88	North American Vertical Datum of 1988
NGS	National Geodetic Survey
OPUS	Online Positioning User Service
PVC	polyvinyl chloride
USGS	United States Geological Survey
VLM	vertical land motion

Units of Measurement / Values

ft	feet
in.	inch
m	meters
mm/yr	millimeters per year
gal/d	gallons per day
%	percent
±	plus/minus
>	greater than
<	less than

LAND SUBSIDENCE MONITORING TO ASSESS POTENTIAL EFFECTS OF GROUNDWATER WITHDRAWALS FROM COASTAL PLAIN AQUIFERS IN MARYLAND

FALL, 2020 SURVEY

by

Thomas Ulizio

KEY RESULTS

Ellipsoid heights at seven 3D survey marks were determined by GPS for comparison with previous measurements to help determine potential changes resulting from groundwater withdrawals in the coastal plain sediments of Maryland. Initial elevations were also determined by GPS for two additional marks, Money Stump (MSTP) and Peter's Neck (PTNK), installed in 2019 and 2020, respectively. The GPS campaign was conducted from October 5 to October 9, 2020 at marks Arnold (ARNO), Broad Creek (BROA), and Crofton Meadows (CROF) well fields, Cove Point (COV1), Lexington Park (LEX1), Rosaryville State Park (ROS1), and Waldorf (WAL1). PTNK was monitored from October 7 to October 10, 2020. MSTP was monitored from October 26 to October 29. GPS data were processed using the National Geodetic Survey's online OPUS Projects utility to determine ellipsoid heights referenced to the International Terrestrial Reference Frame 2014. These data were processed in conjunction with 21 years of GPS data for marks ARNO, BROA, and CROF, and 4 years of GPS data for rod marks COV1, LEX1, ROS1, and WAL1, to assess changes in ellipsoid heights over time. GPS data from the two additional marks, MSTP and PTNK, were processed to establish a baseline ellipsoid height and lateral position for future monitoring. Processed results indicate a trend of decreasing ellipsoid heights ranging from 2.3 to 3.1 millimeters per year over the 21-year period of record (1999 to 2020) and 2.3 to 7 millimeters per year over the 5-year period of record (2016 to 2020). The results also show a clear and consistent northwest shift in mark location, coinciding with the movement of the North American Plate. Land subsidence velocities were interpolated for the State of Maryland using the survey data in conjunction with vertical velocity data from continuously operating reference stations published by the National Geodetic Survey. The interpolated subsidence map shows greater subsidence in unconsolidated sediments of the Maryland Coastal Plain. Assuming the background subsidence rate attributable to glacial isostatic adjustment comprises part of the subsidence rate in the Maryland Coastal Plain region, an additional 1.35 mm/yr. of subsidence on average is occurring that is possibly due to groundwater withdrawal.

INTRODUCTION

Groundwater has been withdrawn from the coastal plain aquifer systems of Maryland for decades for water supply. The geological formations of the coastal plain are composed of stacked layers of predominantly unconsolidated sediment consisting of gravel, sand, silt, and clay. Sand and gravel layers contain water stored in interstitial pore spaces between the sediment grains with relatively high permeability, forming aquifers. Clay layers, with relatively low permeability, form confining units. Withdrawal of water from confined aquifers has lowered groundwater levels in Maryland's coastal plain aquifer systems (Staley and others, 2020). A lowering of groundwater levels in a confined aquifer corresponds to a decrease in hydrostatic pressure in the interstitial pore spaces of the aquifer sediments and in the adjacent confining units. A decrease in hydrostatic pressure can lead to compaction of unconsolidated sediment and the subsidence of the land surface as the load from overlying sediment increases.

Studies have shown that parts of the Atlantic Coastal Plain region are experiencing elevated rates of land subsidence compared to physiographic provinces west of the Fall Line (Karegar and others, 2016). The Fall Line is a boundary that separates the unconsolidated Atlantic Coastal Plain sediments from the consolidated bedrock of the Piedmont province (fig. 1). Two dominant processes responsible for the elevated land surface subsidence rates include the collapse of the forebulge of the former Laurentide Ice Sheet due to glacial isostatic adjustment (GIA) and land subsidence due to decreases in hydrostatic pressure in unconsolidated sediments of the Atlantic Coastal Plain in response to groundwater withdrawal (Eggleston and Pope, 2013; Johnson and others, 2017). Land subsidence rates attributable to GIA processes in the Atlantic Coastal Plain region of Maryland have been reported to be as high as 1.1 millimeters per year (mm/yr) (Park and others, 2002) and around 1 mm/yr in the Lower Chesapeake Bay region of Virginia. (Engelhart and others, 2009). Land subsidence rates attributable to groundwater withdrawals from the Potomac Group aquifer system in the Lower Chesapeake Bay region (Franklin and Suffolk, Virginia) have been reported in the range of 1.5 to 3.7 mm/yr (Davis, 1987; Pope and Burbey, 2004).

Land Subsidence due to groundwater withdrawals in the coastal plain region of Maryland has the potential to increase as groundwater withdrawals expand to supply a growing population. Though not likely to directly cause engineering problems, land subsidence related to groundwater withdrawal could amplify the effects of tidal flooding in bayside and coastal communities as sea levels rise in the future. This may be especially problematic for the survival of wetlands and their associated ecology vulnerable to the impacts of sea-level rise. Beginning in 2019, Maryland Geological Survey (MGS) with funding support from the U.S. Geological Survey (USGS) joined a collaborative effort headed by the USGS and including National Geodetic Survey (NGS), Virginia Tech, and others, to monitor land subsidence in the mid-Atlantic region with special emphasis on potential effects to wetland ecology.

OBJECTIVE AND SCOPE OF WORK

The objective of this work is to monitor permanent survey marks for potential land subsidence resulting from groundwater withdrawals in Southern Maryland and the Eastern Shore of Maryland. The addition of the Money Stump and Peter's Neck marks has expanded the network of high-integrity survey marks. Most of the marks are located in areas of high groundwater withdrawals and corresponding deep cones of depression in Anne Arundel County and Southern Maryland. For comparison, a mark was established in an area of relatively low groundwater withdrawal in Southern Prince George's County, Maryland. The Money Stump and Peter's Neck marks, located in the Blackwater National Wildlife Refuge, provide additional vertical height control in sensitive wetland areas. It is intended that GPS elevation surveys will be conducted at yearly intervals (in the fall) at the established marks to monitor potential changes in height.

BACKGROUND

Groundwater withdrawals from unconsolidated, confined coastal plain aquifers in Maryland have resulted in significant drawdown of groundwater levels. Withdrawals of groundwater are expected to increase to supply a growing population, further drawing down groundwater levels. As drawdown increases, a reduction in hydrostatic pressure in the aquifer systems results in an increased load on the sediment, potentially leading to compaction and subsidence of the land surface. Land subsidence ranging from 1.5 to 3.7 mm/yr has occurred in the lower Chesapeake Bay region of Virginia, attributable in part to groundwater withdrawals from the Potomac Group aquifer

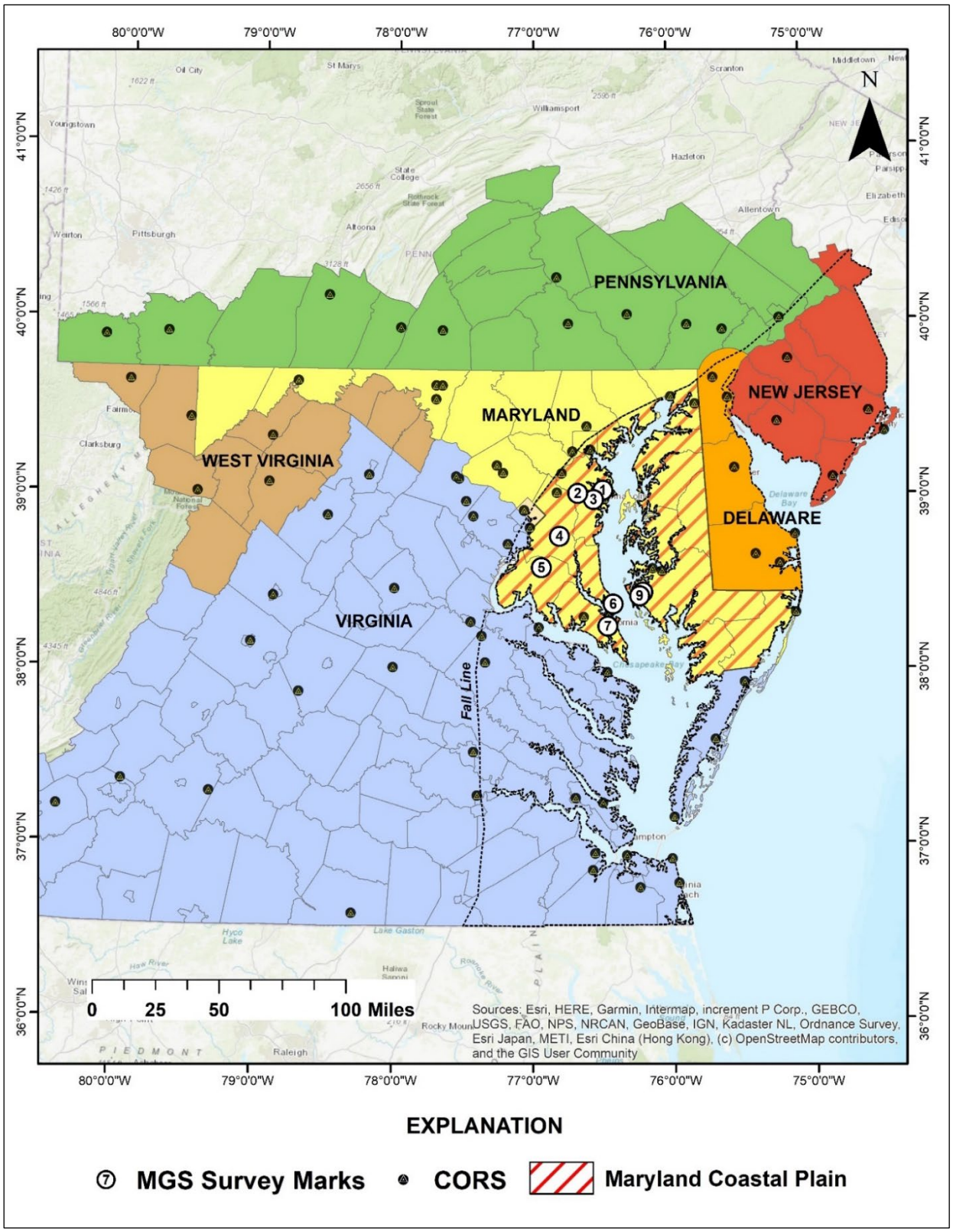

Figure 1. Location of study area, MGS survey marks and CORS stations used in data processing. MGS survey marks are ARNO (1), CROF (2), BROA (3), ROS1 (4), WAL1 (5), COV1 (6), LEX1 (7), PTNK (8), and MSTP (9).

system (the equivalent of the Patapsco and Patuxent aquifer systems in Maryland) (Davis, 1987; Eggleston and Pope, 2013).

Initially, subsidence of the land surface attributable to groundwater withdrawals would be minimal because the sediments were subjected to greater overburden pressures (preconsolidated) in the geologic past caused by the weight of younger sediments that have since been removed through erosional processes (Davis, 1987; Obermeier, 1984). This is particularly true in older lower Cretaceous deposits. In order to induce land subsidence by way of groundwater withdrawal, the grain-to-grain load must increase beyond the stress imparted by sediments prior to consolidation. It has been suggested that a head loss of at least 20 meters (m) (66 feet) in fine-grained sediments of the Atlantic Coastal Plain is necessary before subsidence can occur (Davis, 1987). In some areas of Southern Maryland, groundwater levels have declined as much as ~70 m (230 ft) from estimated pre-pumping levels in response to groundwater withdrawals (Drummond, 2007). This decline in groundwater levels exceeds the head loss of 20 m suggested by Davis (1987) for fine-grained sediments necessary to induce land subsidence.

As part of the land subsidence monitoring effort initiated by MGS, the Maryland State Highway Administration (Division of Plats and Surveys) had monitored survey marks at Arnold, Broad Creek, and Crofton Meadows from 1994-2015 to determine the spatial relationship between the three well sites and a stable monument in the Piedmont physiographic province in Maryland. The stable monument (GORF) is located at Howard High School in Columbia, Maryland. The Maryland State Highway Administration used a variety of GPS receivers and antennas over the duration of their monitoring efforts. GPS occupations were conducted for 5-6 hours over three consecutive days. GPS observations were reduced to vectors using the Topcon Tools[1] software package and then adjusted to the North American Datum of 1983 (NAD83) and the North American Vertical Datum of 1988 (NAVD88). The stable monument in Columbia, MD was used as a reference for adjustments in NAVD88. Data were processed for geoid heights using the GEOID 2003 model which converts ellipsoid heights derived from GPS observations to NAVD88 compatible values. Annual reports describing the data collection and processing are on file at MGS. In 2016, MGS collaborated with the National Geodetic Survey to assume the GPS monitoring of Arnold, Broad Creek, and Crofton Meadows along with additional marks at Cove Point (COV1), Lexington Park (LEX1), Rosaryville State Park (ROS1), and Waldorf (WAL1). GPS data was initially processed by MGS in International GNSS Services 2008 reference frame (IGS08) for ellipsoid heights. Data presented here has been reprocessed for years 1999-2020 in International Terrestrial Reference Frame 2014 (ITRF14). In 2019, a systematic effort began in collaboration with USGS, NGS, Virginia Tech, and others, to determine rates of vertical land motion in the mid-Atlantic region. This effort encompasses the entire Chesapeake Bay region, from the Tidewater region of Southeast Virginia to the Northern Chesapeake and Delaware. In total, 56 survey marks are being monitored every October for five years, 2019-2023. Each mark is continuously occupied for a minimum of 72 hours using NGS-calibrated tripods to ensure accurate antenna reference positions are used in data processing. The collaborative effort monitors a variety of marks including extensometers, deep rod marks, concrete monuments, surface elevation tables, disks embedded in massive structures, and buildings (USGS, 2020).

LOCATION OF STUDY AREA

The study area is in the Coastal Plain Physiographic Province of Maryland (fig. 1). All survey mark sites are located on public property (County, State, or Federally owned), except for the Cove Point site, which is owned by Dominion LNG, LP and managed by Calvert County Department of Parks and Recreation. Two survey marks, PTNK and MSTP, are in the Blackwater National Wildlife Refuge in Dorchester County.

DESCRIPTION OF NEWLY INSTALLED SURVEY MARKS

Two 3D deep rod marks were installed at the Blackwater National Wildlife Refuge in Dorchester County, Maryland to expand the land subsidence monitoring network. The marks, Money Stump (MSTP) and Peter's Neck (PTNK), were installed using materials and methods consistent with NGS standards (Floyd, 1978). Prior to installing the mark rod, a 14-inch (in.) diameter hole was dug to a depth of 22 in. by hand spade and digging bar, then deepened to 44 in. using a 5-in. diameter hand auger. A 9/16-in. stainless steel rod with a drive point was

[1] The use of company names, trade names, or product names in this report is for identification purposes only and does not constitute endorsement by the Maryland Geological Survey.

centered in the open hole and driven to refusal using a 70-pound electric percussion hammer delivering 950 blows per minute with 55 ft-pounds of impact energy. Refusal was reached when continuous hammering resulted in less than 1 ft of penetration over a 1-minute interval. The rod was cut or driven so that the top was approximately 3 in. below the land surface. A greased plastic sleeve was installed over the rod and the hole was backfilled with clean, medium-grain sand to a depth of approximately 20 inches. A 6-in. PVC protective casing with a weatherproof cap was installed over the rod/sleeve assembly and the annular space outside the PVC casing was filled with cement. The inside of the PVC casing was filled to within approximately 6 in. of the top with sand.

Descriptions of marks ARNO, BROA, and CROF are given in Mack (1995) and descriptions of marks COV1, LEX1, ROS1, and WAL1 are given in Andreasen (2016).

Money Stump

The Money Stump deep rod mark (MSTP), installed August 20, 2019, is located in the Blackwater National Wildlife Refuge in Dorchester County, Maryland (figs. 2 and 3). The mark is located at the end of an unnamed access road leading to the marsh. The access road intersects Smithville Road to the West and terminates in the wetland area north of Beaverdam Creek. The surficial sediment encountered in the dug hole at the site consists of approximately 4 ft of tough, gray clay with silt. Refusal at the site was reached at 32 ft. The mark likely extended into Pleistocene-age paleochannel deposits (DeJong and others, 2015). The sky view is partially obstructed to the north and east by a forested area of mature loblolly pines and other mature trees. The sky view is relatively unobstructed to the west as the forested area opens to a wetland area of reed grasses and phragmites. The sky view to the south is unobstructed. Obstructions to the north and east potentially constrain GPS satellite geometry.

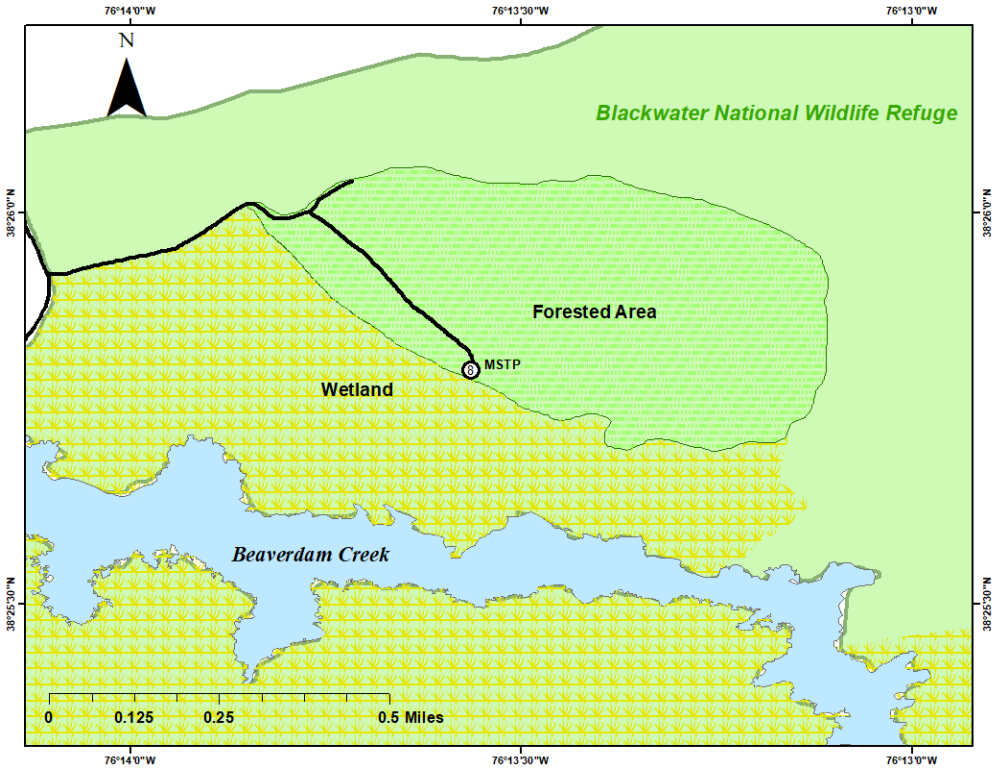

Figure 2. Location of the Money Stump survey mark (MSTP).

Figure 3. Installation of the Money Stump survey mark (MSTP).

Peter's Neck

The Peters Neck deep rod mark (PTNK), installed September 25, 2020, is located in Blackwater National Wildlife Refuge in Dorchester County, Maryland (figs. 4 and 5). The mark is located along the access road, Harrisville Road, leading to the marsh. The surficial sediment encountered in the dug hole at the site consists of approximately 4 ft of slightly silty light gray clay containing root material, fining downward to a darker, gray clay.

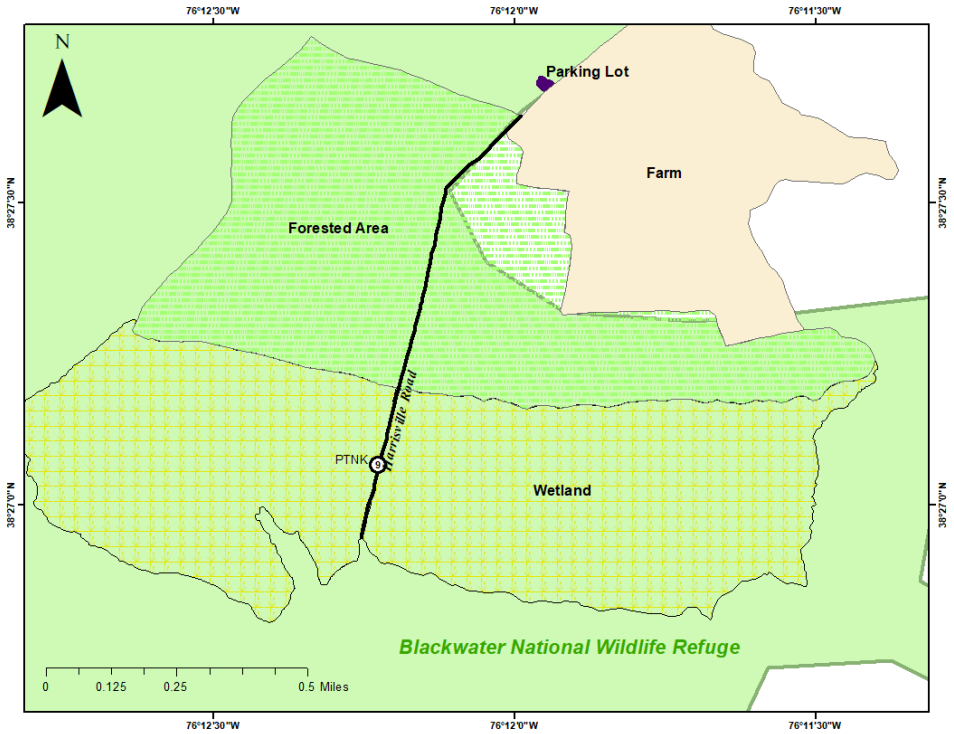

Figure 4. Location of the Peter's Neck survey mark (PTNK).

Refusal at the site was reached at 40.5 ft. The mark likely extended into a Pleistocene-age paleochannel deposit (Fleming and others, 2011; De Jong and others, 2015). The sky view at the site is partially obstructed to the west by phragmites standing 6-8 ft in height. These phragmites are within about 3 ft of the mark. The sky view is partially obstructed to the north and east by phragmites standing 6-8 ft in height. The sky view is less obstructed to the south as Harrisville Road continues. There are some phragmites to the south as well as a lone stand of mature loblolly pines, potentially constraining GPS satellite geometry.

Figure 5. Installation and monitoring of the Peter's Neck survey mark (PTNK).

GPS OCCUPATION (2020) AND DATA PROCESSING

GPS occupations of the ARNO, BROA, CROF, COV1, LEX1, ROS1, and WAL1 survey marks were conducted by MGS from October 5 to October 9, 2020. Survey mark PTNK was occupied by MGS from October 7 to October 10, 2020. Survey mark MSTP was occupied by the U.S Geological Survey (USGS) from October 26 to October 29, 2020. Occupations were conducted using dual frequency (L1/L2) Trimble NetR9 or Trimble 5700 receivers with Zephyr 3 or Ashtech choke ring geodetic antennas[2]. Antennas (oriented north) were attached to fixed height 2-meter tripods calibrated by NGS prior to the occupation. GPS readings were recorded at a 30 second sampling rate.

GPS data were processed using the NGS's OPUS Projects online utility (https://geodesy.noaa.gov/OPUS-Projects/OpusProjects.shtml) to determine horizontal positions and ellipsoid heights of survey marks. Ellipsoid heights were used as opposed to orthometric heights in order to avoid potential loss of accuracy associated with geoid models. Data processing parameters specified by OPUS Projects included a piecewise linear tropospheric model with an interval of 7,200 seconds, an elevation cutoff of 15 degrees, and normal constraint weights. Data were processed in multiple sessions of simultaneous occupation that correspond to GPS day and Continuously Operating Reference Station (CORS) configuration (app. A). Following session processing, a network adjustment was performed in OPUS Projects using session processing results that met data quality thresholds set by OPUS Projects (app. B). The results of these processing steps are horizontal positions and ellipsoid heights for each mark.

[2] The use of company names, trade names, or product names in this report is for identification purposes only and does not constitute endorsement by the Maryland Geological Survey.

Prior data processing of historical GPS data by MGS was done in the International GNSS Service 2008 (IGS08) reference frame for data collected by the Maryland State Highway Administration (1999-2015). That data was reprocessed for this report in ITRF14. The location of all MGS marks and CORS stations used in OPUS session processing are shown in Figure 1. MGS marks occupied in the Fall 2020 campaign are labeled in figures 1 and 9 as numbers 1 through 9: ARNO (1), CROF (2), BROA (3), ROS1 (4), WAL1 (5), COV1 (6), LEX1 (7), PTNK (8), and MSTP (9).

Ellipsoid Heights

Ellipsoid heights for survey marks ARNO, BROA, and CROF were computed using OPUS Projects (fig. 6). Over the 21-year period of record, ellipsoid heights decreased by 0.07 m at ARNO, 0.049 m at BROA, and 0.047 m at CROF. A linear trendline was fitted to the ellipsoid height data. The slope of the linear trendline is reported as the vertical land subsidence rate for the given mark. Over the 21-year period of record, the vertical subsidence rates were 3.1 mm/yr at ARNO, 2.3 mm/yr at BROA, and 2.5 mm/yr at CROF. Ellipsoid heights computed in OPUS Projects at marks COV1, LEX1, ROS1, and WAL1 are shown in Figure 7. Over the five-year period of record, the ellipsoid heights decreased by 0.002 m at COV1, 0.003 m at LEX1, and 0.019 m at WAL1. A linear trendline was fit to the ellipsoid height data. The slope of the linear trendline is reported as the vertical land subsidence rate for the given mark. Over the five-year period of record, the vertical subsidence rates were 3.1 mm/yr at COV1, 0.7 mm/yr at LEX1, 2.3 mm/yr at ROS1, and 7 mm/yr at WAL1.

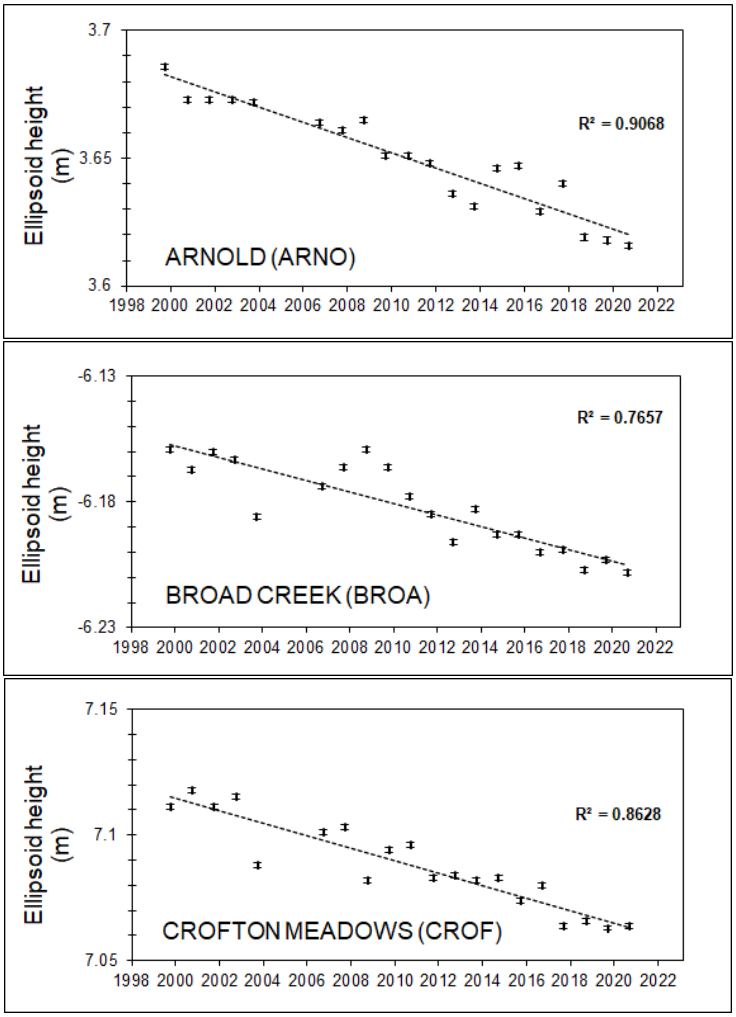

Figure 6. Ellipsoid heights at MGS survey marks Arnold (ARNO), Broad Creek (BROA), and Crofton Meadows (CROF) from 1999-2020.

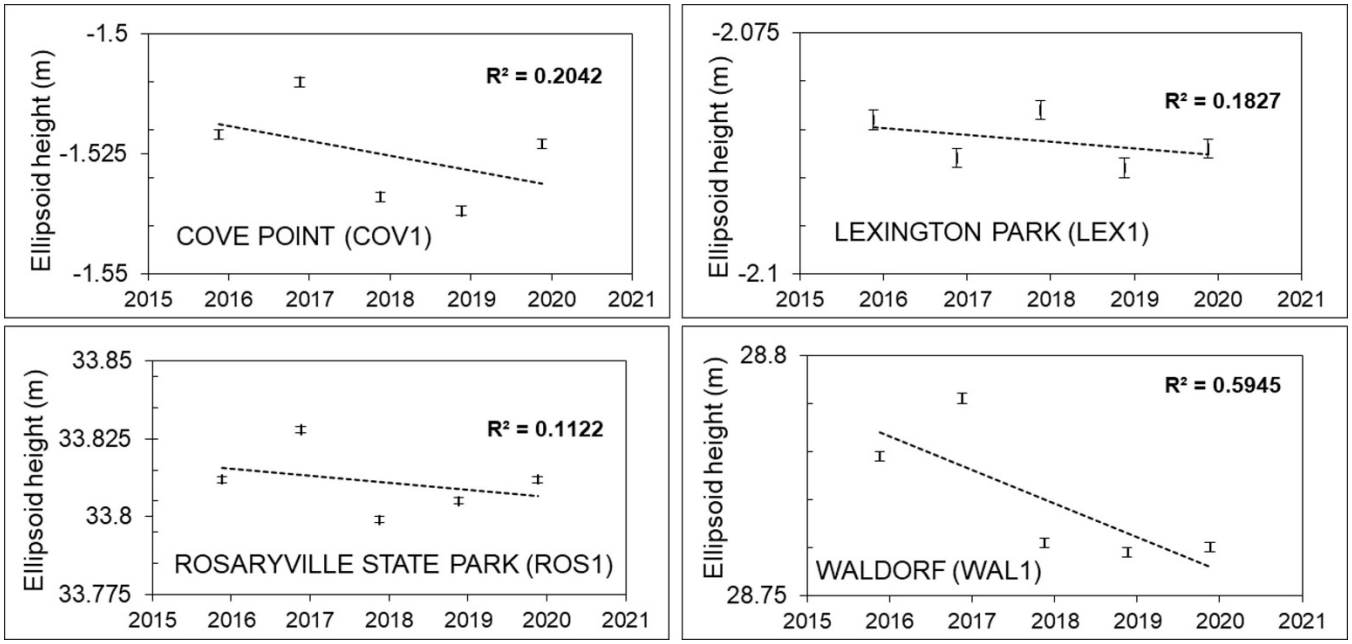

Figure 7. Ellipsoid heights at MGS survey marks Cove Point (COV1), Lexington Park (LEX1), Rosaryville State Park (ROS1), and Waldorf (WAL1) from 2016-2020.

The ellipsoid heights at marks MSTP and PTNK were determined to be -35.640 m and -36.043 m respectively. These data are the first recorded for these marks and will serve as a baseline to which future measurements will be compared.

Horizontal Movement of Survey Marks

Processing results from OPUS Projects allows for the analysis of the horizontal movement of survey marks. The direction, length, and rate of horizontal movement were computed by mapping both the initial mark positions and the 2020 mark positions in an ESRI[3] ArcMap GIS project (app. C). The length of movement was computed using the ArcMap distance measuring tool and the direction of movement was computed using the COGO (Coordinate Geometry) editing tool. The horizontal movement of MGS marks are shown in Figure 8. All marks moved to the northwest over the periods of record with reference to the center of the Earth (ITRF14).

Over the period of record 1999-2020, ARNO moved 323.19 mm, BROA moved 304.50 mm, and CROF moved 304.08 mm. Over the period of record 2016-2020, COV1 moved 66.60 mm, LEX1 moved 62.50 mm, ROS1 moved 82.80 mm, and WAL1 moved 59.40 mm. The direction of movement was 72.45° west of north at ARNO, 73.62° west of north at BROA, 73.29° west of north at CROF, 68.33° west of north at COV1, 73.39° west of north at LEX1, 55.43° west of north at ROS1, and 70.29° west of north at WAL1.

[3] The use of company names, trade names, or product names in this report is for identification purposes only and does not constitute endorsement by the Maryland Geological Survey.

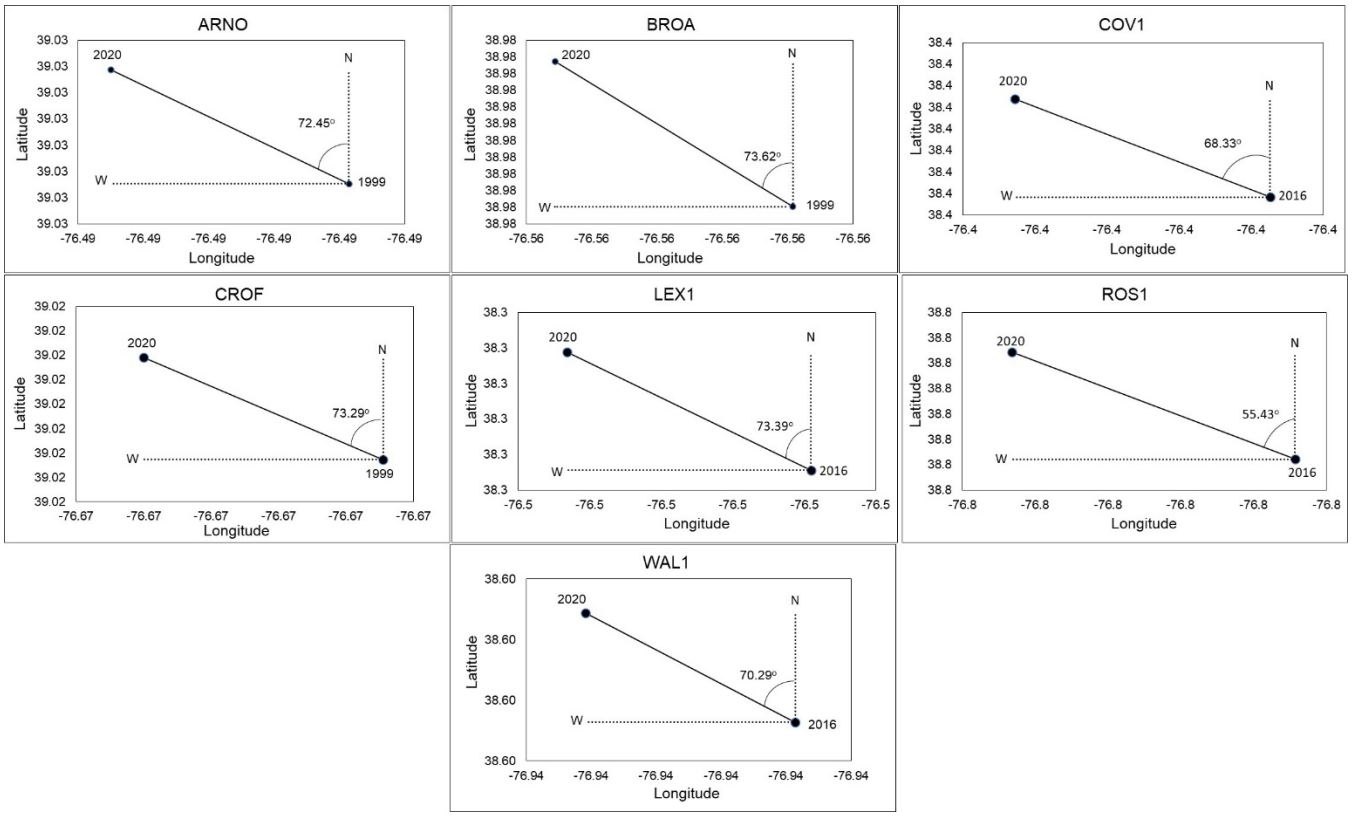

Figure 8. Horizontal movement of MGS survey marks.

Regional Land Subsidence

The rates of change in ellipsoid heights at MGS marks were used in an ESRI GIS ArcMap project to produce an interpolated map of land subsidence within the state of Maryland (fig. 9). Ellipsoid height data for MGS marks MSTP and PTNK were not included in this interpolation. CORS stations used in the OPUS Projects processing for MGS marks as well as other selected CORS stations throughout the mid-Atlantic region were included in the interpolation (app. D). In total, vertical velocity data at 7 MGS marks and 89 CORS stations were used to create a regional interpolation. The extent of the regional interpolation is shown by the colored areas in Figure 1 and covers portions of New Jersey, Pennsylvania, and West Virginia as well as all of Maryland, Delaware, Virginia, and Washington D.C. Only the portions within Maryland are presented herein in the land subsidence map. Because marks MSTP and PTNK were only recently established and therefore lacked historical data, they were not included in the interpolation.

Vertical velocity data for CORS stations were retrieved from NGS data sheets. From these point data, an interpolated regional vertical velocity raster was generated using the Inverse Distance Weighted function in the ArcGIS Geostatistical Analyst Toolbox. Positive vertical velocity values indicate subsidence while negative values indicate uplift. For the purposes of this study, the results of the regional interpolation were clipped to fit the boundary of the state of Maryland. Regional data from CORS sites are important for interpolating vertical velocities in the state of Maryland because the proximity of CORS stations located in Pennsylvania, Virginia, and West Virginia allow for better interpolation of areas in Maryland that lack CORS data. The vertical velocity rates are mapped alongside the physiographic provinces to discern any spatial trends in subsidence as it relates to the underlying geology.

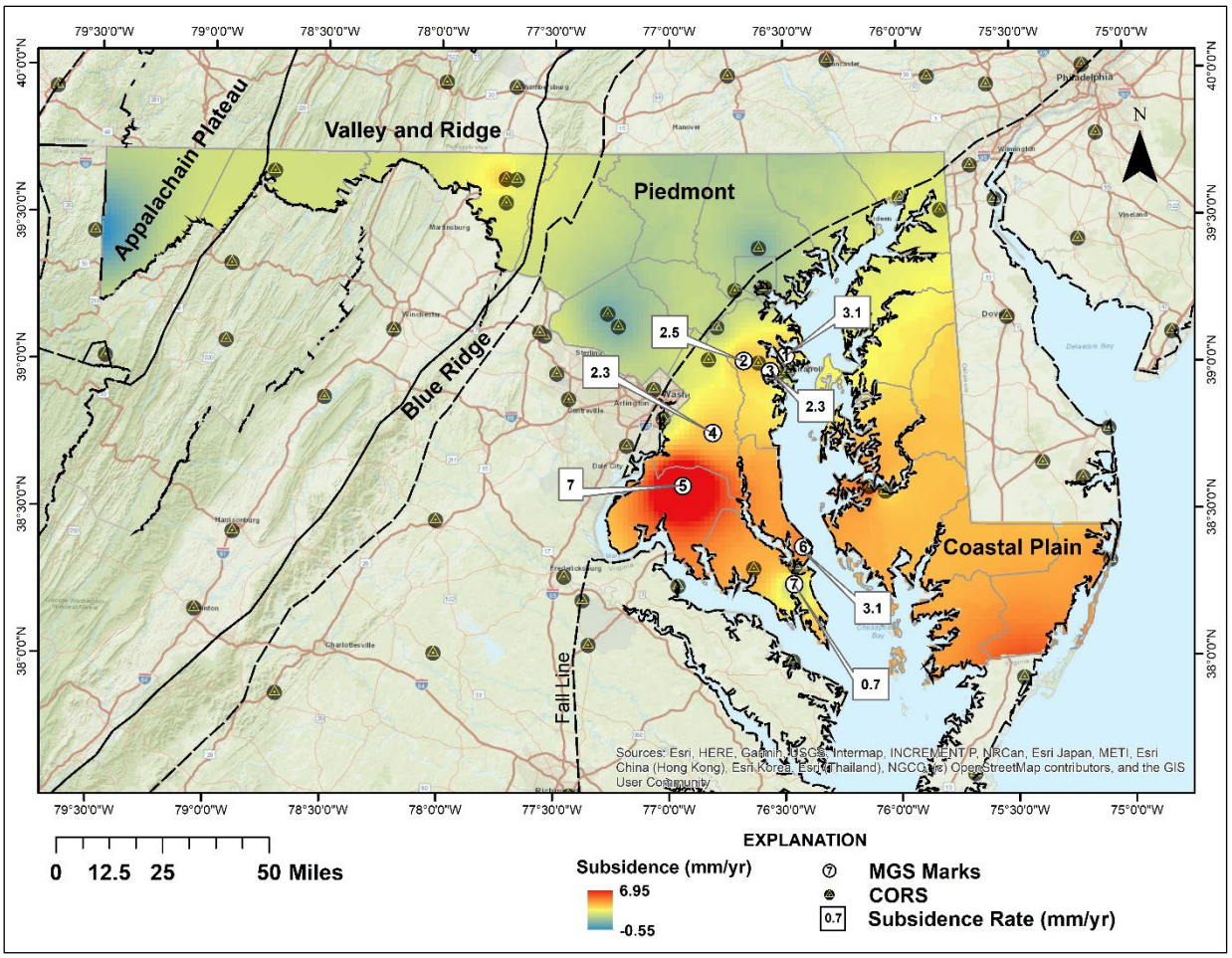

Figure 9. Interpolated vertical velocity rates for the State of Maryland.

Discussion

Computed vertical velocity rates for marks COV1, LEX1, ROS1, and WAL1 may not capture the true rate of subsidence, as the computed rates are limited by the shorter duration (2016-2020) of data collection and processing compared to those for marks ARNO, BROA, and CROF (1999-2020). The longer periods of record for ellipsoid height data at marks ARNO, BROA, and CROF factor out the year-to-year variability that is inherent in OPUS processing (fig. 6). OPUS processing results may show an increase in ellipsoid heights from one year to the next, while capturing the long-term trend in decreasing ellipsoid heights over the 21-year period of record. Marks COV1, LEX1, ROS1, and WAL1 show a similar year-to-year variability in OPUS processing results but the five-year period of record does not capture the trend of decreasing ellipsoid heights in the same way as the long-established marks. Therefore, a linear trendline fit to this shorter time series of data (and the slope of this linear trendline, reported as the vertical velocity rate) does not capture the subsidence trends as well as longer time series data. This is illustrated in the smaller calculated coefficients of determination (R^2) for COV1, LEX1, ROS1, and WAL1 data (figs. 6 and 7). MGS mark LEX1 is representative of the limitations attributed to relatively short data time series. The slope of the linear trendline of ellipsoid heights resulted in a subsidence rate of 0.7 mm/yr., much lower than surrounding areas. This limitation in data availability is reflected in the regional vertical velocity interpolation (fig. 9).

Vertical velocity data and the interpolation of the 96 data points reveals spatial trends in land subsidence. Though both regions show overall subsidence, the interpolated subsidence rates are higher in the unconsolidated sediments of the coastal plain of Maryland compared to the physiographic provinces underlain by consolidated

bedrock to the west of the Fall Line (fig. 9). The mean subsidence rate of the Maryland Coastal Plain is 2.3 mm/yr, which is comparable and within range of the subsidence rates (1.5-3.7 mm/yr) reported by Davis (1987) and Eggleston and Pope (2013). The mean subsidence rate of the bedrock physiographic provinces is 0.95 mm/yr, which is comparable to the reported rates of Park and others (2002) and Engelhart and others (2009). Assuming the background subsidence rate attributable to GIA (~1 mm/yr) comprises part of the subsidence rate in the Maryland coastal plain, an additional 1.3 mm/yr of subsidence on average is occurring, possibly due to groundwater withdrawal. By classifying the vertical velocity interpolation raster to only symbolize regions of subsidence that exceed one standard deviation above the regional mean subsidence rate (>1.99 mm/yr), we see that this level of subsidence is specific to the Maryland Coastal Plain (fig. 10). This is true except for one area of subsidence exceeding 1.99 mm/yr in the Valley and Ridge province of Western Maryland. Large areas of the Valley and Ridge Province are underlain by carbonate rock that has been subjected to karstification (Brezinski, 2018) and the subsidence in this area may be a result of karst subsidence.

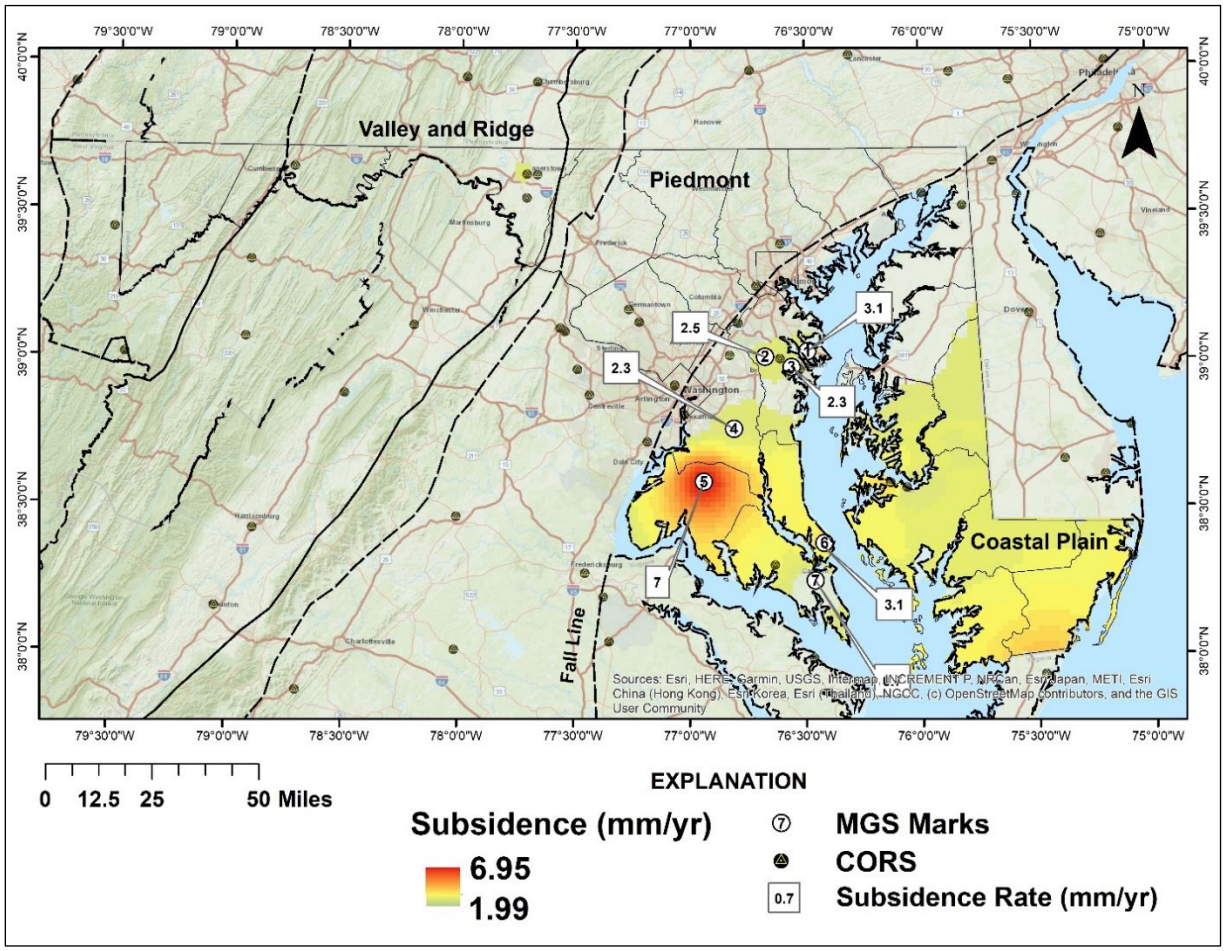

Figure 10. Interpolated vertical velocity rates for areas of subsidence with rates more than one standard deviation above the mean regional vertical velocity rate.

As can be seen from the interpolated subsidence map (fig. 9), subsidence rates are not uniform across the coastal plain of Maryland. The Waldorf, Maryland area shows a much higher subsidence rate compared to the rest of the coastal plain. The aquifer systems of the Waldorf area have experienced extensive groundwater withdrawals. The total withdrawal from aquifer systems near Waldorf has lowered water levels by as much as approximately 230 ft from pre-pumping water levels (Andreasen, 2016). The location of greatest stress to the aquifers caused by withdrawals is illustrated by a composite of water levels in five major aquifers or aquifer systems during the fall of 2013 (Andreasen, 2016) (fig. 11). These aquifers include, from shallowest to deepest, the Aquia, Magothy, Upper Patapsco, Lower Patapsco, and Patuxent. The areas of greatest stress (deepest composite water levels) correspond almost exactly with the location of highest subsidence rates. To a lesser extent, there appears to be spatial overlap between aquifers stressed by withdrawals and subsidence in the central Anne Arundel County area. Discrepancies between expected subsidence and areas of stressed aquifers occur most noticeably at mark LEX1. Lexington Park is at the center of a relatively deep cone of depression in the Aquia aquifer (Staley and others, 2020), yet data from this mark show subsidence rates on the low side and the surrounding areas do not show subsidence rates in excess of one standard deviation above the mean regional subsidence rate. This is possibly related to the data limitations of short time series data described previously, or it may be because the period of greatest drawdown in the Aquia aquifer happened from about 1970 to 2005, before the mark was established. The Easton, Maryland area has also experienced significant drawdown of groundwater levels. One might expect a greater subsidence rate for this area in the vertical velocity interpolation map; however, location-specific data regarding subsidence rates were simply not available for the area. The paucity of vertical velocity data on the Eastern Shore in general acts as a limiting factor in the interpolation of subsidence rates in that area.

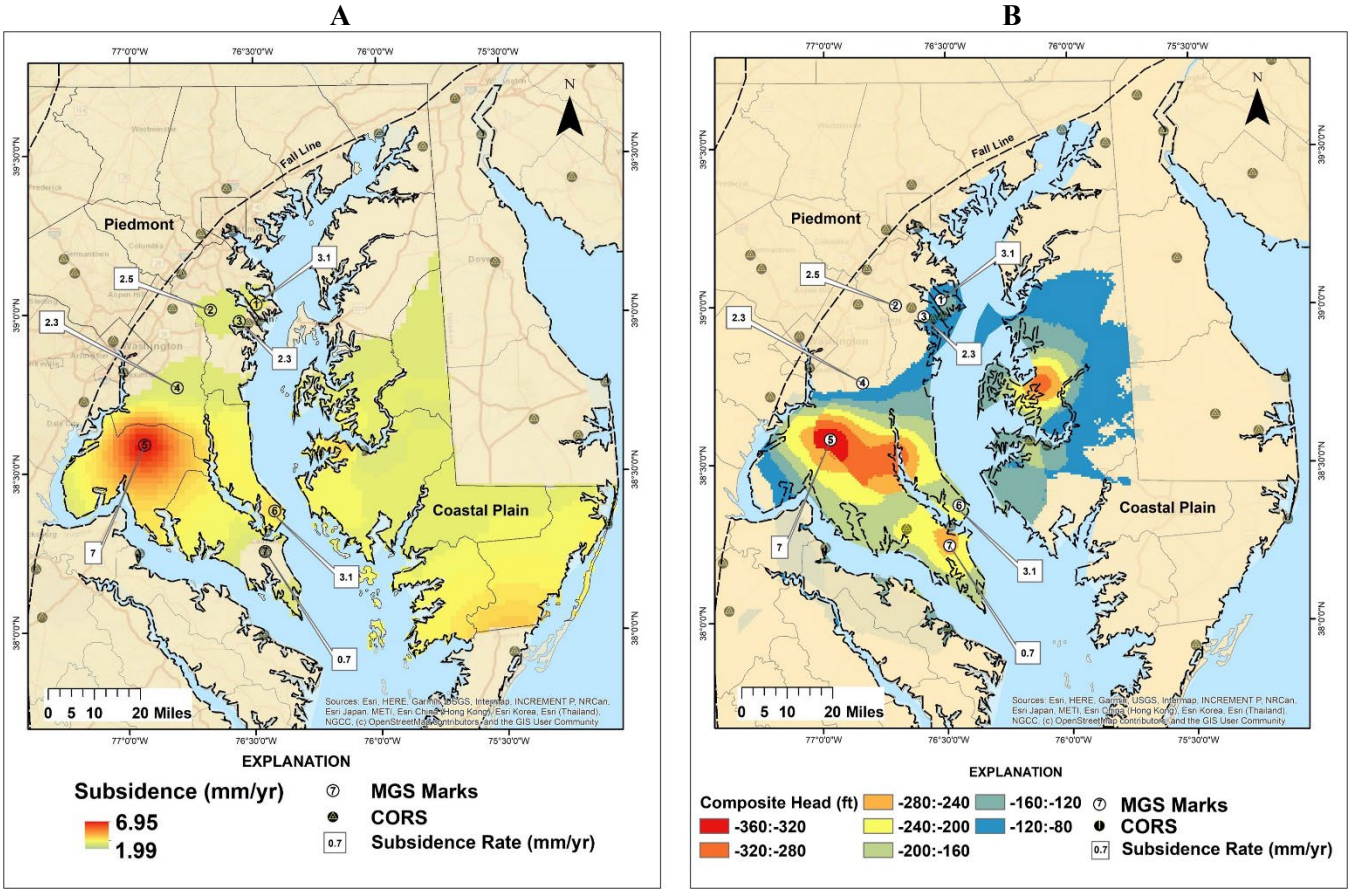

Figure 11. Spatial comparison of: (A) vertical velocities more than one standard deviation above the mean regional subsidence value; and (B) composite water levels from five regional aquifer systems.

An important point to discuss is the variability in OPUS Projects session processing results attributed to specific CORS sites chosen during processing. These session results serve as inputs to the final network adjustment from which ellipsoid heights are calculated. Because of the relatively long time series of GPS data for marks ARNO, BROA, and CROF, it is impossible to maintain consistency in CORS selection during the OPUS Projects processing from year to year. During the 21-year period of record for ARNO, BROA, and CROF, CORS sites were discontinued, new CORS sites were established in the CORS network, and CORS data may not be available for certain years. The CORS sites used in data processing for each year of occupation differed from year to year, depending on the availability of data (app. A). The variation in ellipsoid heights computed for ARNO, BROA, and CROF during session processing for occupation year 2002 is shown in Figure 12 as an example. These plots show the ranges in computed ellipsoid heights derived from session processing for occupation year 2002 (0.016 m at ARNO, 0.025 m at BROA, and 0.027 m at CROF). The interquartile range of the data for occupation year 2002 are 0.007 m at ARNO, 0.007 m at BROA, and 0.008 m at CROF. This can be interpreted as the mid-spread of the data. The middle 50 percent of the computed ellipsoid heights from session processing for occupation year 2002 were as high as 8 mm. This exposes the limitation of using OPUS Projects to measure millimeter scale changes in ellipsoid heights on a year-to-year basis.

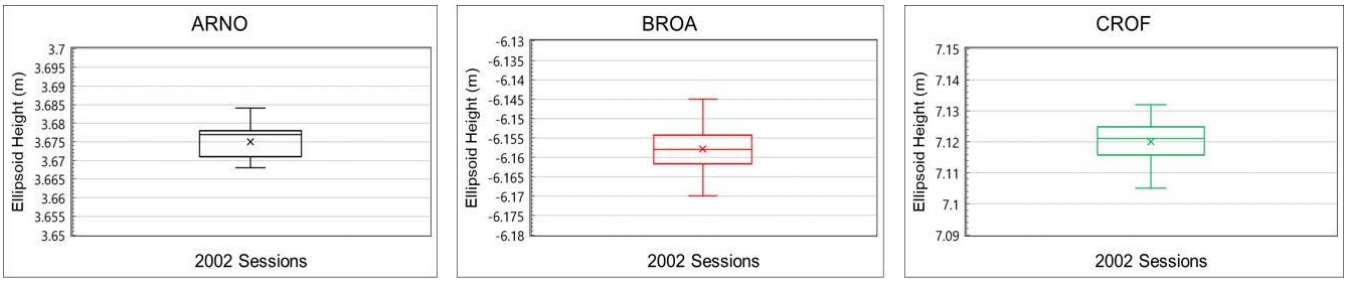

Figure 12. Variability in ellipsoid height outputs from OPUS Projects session processing results for occupation year 2002.

The horizontal movement of survey marks computed in OPUS Projects captures the movement of the North American Plate. Horizontal velocities and directionality of seven of the nine marks (app. C) were compared to computed horizontal velocities and directions of movement of CORS stations in the area. The similarities between computed horizontal velocities and directions for MGS marks in OPUS Projects and the horizontal velocities and directions reported by DeMets and others (2010) and Santamaria-Gomez and others (2012) help to validate the methodology of GPS occupation and processing used in this study's analysis. Though ellipsoid heights computed through OPUS Projects show millimeter scale variance from year to year, the vertical velocities derived from these ellipsoid heights can be considered credible given the similarity in processed horizontal results which used the same methodology.

SUMMARY

Nine 3D survey marks were monitored for potential land subsidence caused by groundwater withdrawals in Southern Maryland. Six of the marks (Arnold [ARNO], Broad Creek [BROA], Crofton Meadows [CROF], Cove Point [COV-1], Lexington Park [LEX-1], and Waldorf [WAL-1]) are in areas of significant groundwater withdrawal where water levels have declined significantly. An additional mark site−Rosaryville State Park [ROS1] in southern Prince George's County−is in an area of relatively low groundwater withdrawals for comparison. Two additional marks were installed in the Blackwater Wildlife Refuge (Money Stump [MSTP] in 2019 and Peter's Neck [PTNK] in 2020) on Maryland's Eastern Shore in part to help assess potential impacts of land subsidence on wetlands. GPS readings were made at all marks in the fall of 2020 to obtain ellipsoid heights. The GPS data were processed using the National Geodetic Survey's OPUS Projects online utility. Ellipsoid height accuracy ranged from 0.002 to 0.003 m.

Vertical velocities were computed from ellipsoid heights for seven of the nine 3D marks. These velocities were

combined with a data set of computed velocities for 82 Continuously Operating Reference Stations (CORS) to generate an interpolated vertical velocity map for the mid-Atlantic region. Comparison of the interpolated subsidence rates with areas of excessive aquifer drawdown showed that areas that have experienced excessive aquifer drawdown in Charles County and Anne Arundel County are also experiencing rates of subsidence greater than one standard deviation above the mean subsidence rate for the state of Maryland.

ACKNOWLEDGEMENTS

Funding support for this project was provided by Anne Arundel County Department of Public Works, Dominion LNG/LP, and the U.S. Geological Survey. Charles Geoghegan, Phillipe Hensel and Ryan Hippenstiel of the National Geodetic Survey facilitated the calibration of survey tripods and the loan of survey equipment. Special thanks to Matt Whitbeck of the U.S. Fish and Wildlife Service (Blackwater National Wildlife Refuge) for providing access for the Money Stump and Peters Neck marks. David Andreasen, Christopher Connallon, and Andrew Staley, all of Maryland Geological Survey, and Allison VanVorst of the Blackwater National Wildlife Refuge, aided with installation of the marks. Assistance in GPS surveying was provided by David Andreasen, Heather Quinn, and Andrew Staley of the Maryland Geological Survey, and David Walters of the U.S. Geological Survey. The report was reviewed by David Andreasen and Andrew Staley.

REFERENCES

Andreasen, D.C., 2016, Establishment of a land subsidence-monitoring network to assess the potential effects of groundwater withdrawals in Southern Maryland, Maryland Geological Survey Open File Report 16-02-01, 38,p.

Brezinski, D.K., 2018, Geology and karst development of the Hagerstown Valley (Great Valley) of Maryland: Maryland Geological Survey Report of Investigations No. 86, 102 p.

Davis, G.H., 1987, Land Subsidence and Sea Level Rise on the Atlantic Coastal Plain of the United States: Environmental Geology and Water Sciences, vol. 10, no. 2, p. 67-80.

DeJong, B., **Bierman, P.R., Newell, W.L, Rittenour, T.M, Mahan, S.A,** 2015, Pleistocene relative sea levels in the Chesapeake Bay region and their implications for the next century, GSA Today, vol. 25, no. 8, p. 4-10.

DeMets, C., Gordon R.G., and Argus D.F., 2010, Geologically current plate motions, Geophysical Journal International, vol. 181, no.1, p. 1-80.

Drummond, D.D., 2007, Water-Supply Potential of the Coastal Plain Aquifers of Calvert, Charles, and St. Mary's Counties, Maryland, with Emphasis on the Upper Patapsco and Lower Patapsco Aquifers: Maryland Geological Survey Report of Investigation 76, 225 p.

Eggleston, J., and Pope, J.,, 2013, Land subsidence and relative sea-level rise in the southern Chesapeake Bay region: U.S. Geological Survey Circular 1392, 30 p.

Engelhart, S.E., Horton, B.P., Douglas, B.C., Peltier, W.R., and Tornqvist, T.E., 2009, Spatial variability of late Holocene and 20th century sea-level rise along the Atlantic coast of the United States: Geology, vol. 37, no.12, p. 1115-1118.

Fleming, B.J., DeJong, B.D., Phelan, D.J., 2011, Geology, Hydrology, and Water Quality of the Little Blackwater River Watershed, Dorchester County, Maryland, 2006-09, USGS Scientific Investigations Report 2011-5054, p. 6-9.

Floyd, Lt. R.P, 1978, NOAA Manual NOS NGS 1: Geodetic bench marks: National Oceanic and Atmospheric Administration, National Geodetic Survey, Rockville, Maryland, 52 p.

Johnson, C.S., Miller, K.G., Browning, J.V., Kopp, R.E., Khan, N.S., Fan, Y., Stanford, S.D., Horton, B.P., 2017, The role of sediment compaction and groundwater withdrawal in local sea-level rise, Sandy Hook, New Jersey, USA: Quaternary Science Reviews, 181, p. 30-42.

Karegar, M.A., Dixon, T.H., and Engelhart, S.E., 2016, Subsidence along the Atlantic Coast of North America: Insights from GPS and late Holocene relative sea level data: Geophysical Research Letters, vol. 43, no. 7, p. 3126–3133.

Obermeier, S.F, 1984, Engineering geology of Potomac Formation deposits in Fairfax County, Virginia and vicinity with emphasis on landslides, *in* S.F Obermeier, ed., Engineering geology and design of slopes for Cretaceous Potomac deposits in Fairfax County, Virginia and Vicinity: U.S Geological Survey Bulletin 1556, p. 5-48.

Park, K.D., Nerem, R.S., Davis, J.L., Schenewerk, M.S., Milne, G.A., and Mitrovica, J.X., 2002, Investigation of glacial isostatic adjustment in the northeast U.S using GPS measurements: Geophysical Research Letters, vol. 29, no. 11, p. 4-1 – 4-4.

Pope, Jason and Burbey, Thomas J., 2004, Multiple-Aquifer Characterization from Single Borehole Extensometer Records: Ground Water, vol. 42, no.1, p. 45-58.

Santamaria-Gomez, A.M., Gravelle, M., Collilieux, X., Guichard, M., Martin Miguez, B., Tiphaneau, P., Woppelmann, G., 2012, Mitigating the effects of vertical land motion in tide gauge records using a state-of-the-art GPS velocity field, Global and Planet Change, vol. 98-99, p. 6-17.

Staley, A.W., Andreasen, D.C., and Marchand, E.H., 2020, Potentiometric surface maps of selected confined aquifers in Southern Maryland and Maryland's Eastern Shore, 2019: Maryland Geological Survey Open File Report 20-02-01, 38 p.

U.S. Geological Survey, 2020, New Crowd Sourcing Will Contribute to Study of Land Subsidence and Sea-Level Rise in the Chesapeake Bay: https://www.usgs.gov/centers/cba/science/new-crowd-sourcing-will-contribute-study-land-subsidence-and-sea-level-rise?qt-science_center_objects=0#qt-science_center_objects. Accessed 6/2020

Appendix A. List of CORS sites used in OPUS Projects data processing.

Year	CORS	Use in OPUS Projects	
		Session Processing	Network Adjustment
1999	ERLA	Troposphere Correction	Unconstrained
	HNPT		Constrained (3D)
	GAIT		Constrained (3D)
	USNA	Hub	Constrained (3D)
	WDC1		Constrained (3D)
2000	ERLA	Troposphere Correction	Unconstrained
	HNPT		Constrained (3D)
	GAIT		Constrained (3D)
	USNA	Hub	Constrained (3D)
	WDC1		Constrained (3D)
2001	ERLA	Troposphere Correction	Unconstrained
	HNPT		Constrained (3D)
	GAIT	Hub	Constrained (3D)
	GODE	Hub	Constrained (3D)
	USNA	Hub	Constrained (3D)
	WDC1		Constrained (3D)
2002	ERLA	Troposphere Correction	Unconstrained
	HNPT		Constrained (3D)
	GAIT	Hub	Constrained (3D)
	GODE	Hub	Constrained (3D)
	USNA	Hub	Constrained (3D)
	WDC1		Constrained (3D)
2003	ERLA	Troposphere Correction	Unconstrained
	HNPT		Constrained (3D)
	GAIT	Hub	Constrained (3D)
	GODE	Hub	Constrained (3D)
	USNA	Hub	Constrained (3D)
	WDC1		Constrained (3D)
2006	ERLA	Troposphere Correction	Unconstrained
	COLA	Troposphere Correction	Unconstrained
	HNPT		Constrained (3D)
	GAIT	Hub	Constrained (3D)
	GODE		Constrained (3D)
	ANP1	Hub	Constrained (3D)
2007	COLA	Troposphere Correction	Unconstrained
	HNPT		Constrained (3D)
	GAIT		Constrained (3D)
	GTS1		Constrained (3D)
	GODE	Hub	Constrained (3D)
	SOL1		Constrained (3D)
	USN3	Hub	Constrained (3D)
2008	COLA	Troposphere Correction	Unconstrained
	BACO	Hub	Constrained (3D
	DENE		Constrained (3D
	GTS1		Constrained (3D
	NRL1	Hub	Constrained (3D
	USN3		Constrained (3D
2009	COLA	Troposphere Correction	Unconstrained
	UMBC		Constrained (3D)
	DENE		Constrained (3D)
	GODE	Hub	Constrained (3D)
	HNPT		Constrained (3D)
	STKR	Troposphere Correction	Unconstrained
2010	COLA	Troposphere Correction	Unconstrained
	BACO	Hub	Constrained (3D)
	NRL1	Hub	Constrained (3D)
	DENE		Constrained (3D)
	GODE	Hub	Constrained (3D)
	GTS1		Constrained (3D)
	USN3	Hub	Constrained (3D)
2011	COLA	Troposphere Correction	Unconstrained
	UMBC		Constrained (3D)
	HNPT		Constrained (3D)
	GODZ	Hub	Constrained (3D)
	GODE		Constrained (3D)
	DENE		Constrained (3D)
	ANP5	Hub	Constrained (3D)
2012	COLA	Troposphere Correction	Unconstrained
	BACO		Constrained (3D)
	HNPT		Constrained (3D)
	DENE		Constrained (3D)
	GODZ	Hub	Constrained (3D)

Appendix A. Continued.

Year	CORS	Use in OPUS Projects	
		Session Processing	Network Adjustment
2012	UMBC		Constrained (3D)
	ANP5	Hub	Constrained (3D)
2013	COLA	Troposphere Correction	Unconstrained
	UMBC		Constrained (3D)
	BACO		Constrained (3D)
	DENE		Constrained (3D)
	GODZ	Hub	Constrained (3D)
	ANP5	Hub	Constrained (3D)
	STKR	Troposphere Correction	Unconstrained
2014	COLA	Troposphere Correction	Unconstrained
	UMBC		Constrained (3D)
	DENE		Constrained (3D)
	GODZ	Hub	Constrained (3D)
	HNPT		Constrained (3D)
	BACO		Constrained (3D)
	ANP5	Hub	Constrained (3D)
2015	COLA	Troposphere Correction	Unconstrained
	UMBC		Constrained (3D)
	DENE		Constrained (3D)
	GODZ	Hub	Constrained (3D)
	HNPT		Constrained (3D)
	BACO		Constrained (3D)
	ANP5	Hub	Constrained (3D)
	ANP6	Hub	Constrained (3D)
	STKR	Troposphere Correction	Unconstrained
2016	COLA	Troposphere Correction	Unconstrained
	UMBC		Constrained (3D)
	DENE		Constrained (3D)
	GODE	Hub	Constrained (3D)
	HNPT		Constrained (3D)
	LOYF	Hub	Constrained (3D)
	BACO		Constrained (3D)
2017	COLA	Troposphere Correction	Unconstrained
	UMBC		Constrained (3D)
	DENE		Constrained (3D)
	GODZ		Constrained (3D)

Year	CORS	Use in OPUS Projects	
		Session Processing	Network Adjustment
2017	HNPT		Constrained (3D)
	BACO		Constrained (3D)
	ANP5	Hub	Constrained (3D)
	ANP6	Hub	Constrained (3D)
	STKR	Troposphere Correction	Unconstrained
2018	COLA	Troposphere Correction	Unconstrained
	UMBC	Hub	Constrained (3D)
	DENE		Constrained (3D)
	GODZ	Hub	Constrained (3D)
	HNPT	Hub	Constrained (3D)
	BACO		Constrained (3D)
	LOY8		Constrained (3D)
	STKR	Troposphere Correction	Unconstrained
2019	COLA	Troposphere Correction	Unconstrained
	UMBC	Hub	Constrained (3D)
	DENE		Constrained (3D)
	GODZ	Hub	Constrained (3D)
	HNPT	Hub	Constrained (3D)
	BACO		Constrained (3D)
	LOY8	Hub	Constrained (3D)
	STKR	Troposphere Correction	Unconstrained
2020	STKR	Troposphere Correction	Unconstrained
	UMBC	Hub	Constrained (3D)
	BACO		Constrained (3D)
	DENE		Constrained (3D)
	GODE		Constrained (3D)
	GODZ	Hub	Constrained (3D)
	LOYO		Constrained (3D)
	WDC5		Constrained (3D)

Appendix B. OPUS Projects network adjustment for the 2020 GPS occupation.

```
                NGS OPUS-Projects 4.11 NETWORK ADJUSTMENT REPORT
                ===============================================

 All coordinate accuracies reported here are 1x the formal
 uncertainties from the solution. For additional information:
 geodesy.noaa.gov/OPUS/Using_OPUS-Projects.html#accuracy

 These positions were computed without any knowledge by the National
 Geodetic Survey regarding the equipment or field operating procedures used.

 SUBMITTED BY:                   thomas.ulizio
 SOLUTION FILE NAME:             network-AAC2020_GeoMin18.sum
 SOLUTION SOFTWARE:              GPSCOM(2008.25)
 SOLUTION DATE:                  2020-11-25T20:41:24 UTC
 STANDARD ERROR OF UNIT WEIGHT: 0.756
 TOTAL NUMBER OF OBSERVATIONS:  1779637
 TOTAL NUMBER OF MARKS:         15
 CONSTRAINED MARKS:             7 HORIZONTAL, 0 VERTICAL
 baco N39:23:58.03744 W076:36:24.44316  128.305m        NAD_83(2011) @ 2010.0000
 baco         0.12cm           0.11cm     0.12cm        NEU SIGMAS
 dene N39:40:36.24965 W075:44:34.82897    6.545m        NAD_83(2011) @ 2010.0000
 dene         0.12cm           0.10cm     0.13cm        NEU SIGMAS
 gode N39:01:18.18970 W076:49:36.57471   15.784m        NAD_83(2011) @ 2010.0000
 gode         0.12cm           0.12cm     0.12cm        NEU SIGMAS
 godz N39:01:18.18970 W076:49:36.57471   15.784m        NAD_83(2011) @ 2010.0000
 godz         0.13cm           0.07cm     0.13cm        NEU SIGMAS
 loyo N38:03:00.62625 W077:20:51.17400   43.177m        NAD_83(2011) @ 2010.0000
 loyo         0.12cm           0.10cm     0.12cm        NEU SIGMAS
 umbc N39:15:24.36082 W076:42:41.46870   65.940m        NAD_83(2011) @ 2010.0000
 umbc         0.13cm           0.08cm     0.13cm        NEU SIGMAS
 wdc5 N38:55:14.00162 W077:03:58.72342   60.266m        NAD_83(2011) @ 2010.0000
 wdc5         0.12cm           0.12cm     0.12cm        NEU SIGMAS

 START TIME:                     2020-10-05T00:00:00 GPS
 STOP TIME:                      2020-10-09T23:59:30 GPS
 FREQUENCY:                      L1-ONLY TO ION-FREE [BY BASELINE LENGTH]
 OBSERVATION INTERVAL:           30 s
 ELEVATION CUTOFF:               15 deg
 TROPO INTERVAL:                 7200 s [PIECEWISE LINEAR PARAMETERIZATION]
 DD CORRELATIONS:                ON

     INCLUDED SOLUTION             RMS    SOFTWARE         RUN DATE
 ------------------------------------------------------------------------------
  1) 2020-279 A_UMBC             1.4 cm  page5(2008.25)   2020-11-25T15:53 UTC
  2) 2020-280 A                  1.3 cm  page5(2008.25)   2020-11-25T15:47 UTC
  3) 2020-280 A_UMBC2            1.4 cm  page5(2008.25)   2020-11-25T20:38 UTC
  4) 2020-281 A                  1.3 cm  page5(2008.25)   2020-11-25T15:47 UTC
  5) 2020-281 A_UMBC             1.5 cm  page5(2008.25)   2020-11-25T20:29 UTC
  6) 2020-282 A                  1.4 cm  page5(2008.25)   2020-11-25T15:48 UTC
  7) 2020-282 A_UMBC             1.5 cm  page5(2008.25)   2020-11-25T20:30 UTC
  8) 2020-283 A_UMBC             1.4 cm  page5(2008.25)   2020-11-25T20:31 UTC

   BASELINE      LENGTH         RMS       OBS   OMITTED    FIXED IN SOLUTION(S)
 ------------------------------------------------------------------------------
  gode-godz      0.000 km      0.3 cm    56103     0.3%    99.8%    2, 4, 6
  crof-godz     13.195 km      1.3 cm    49507     9.3%    98.7%    2, 4, 6
  baco-umbc     18.235 km      1.3 cm    92853     1.9%    99.2%    1, 3, 5,...
  wdc5-godz     23.598 km      1.1 cm    54041     0.5%    99.4%    2, 4, 6
  broa-godz     23.651 km      1.5 cm    51697     6.4%    98.5%    2, 4, 6
  crof-umbc     26.798 km      1.5 cm    66021     8.1%    97.8%    1, 3, 5,...
```

Appendix B. Continued.

```
 ros1-godz     27.469 km      1.7 cm    27749    15.8%    98.1%    2, 4
 godz-umbc     27.934 km      1.4 cm   149251     0.7%    99.4%    1, 2, 3,...
 gode-umbc     27.934 km      1.3 cm    93883     0.3%    98.9%    1, 3, 5,...
 arno-godz     29.173 km      1.3 cm    52849     4.9%    99.0%    2, 4, 6
 arno-umbc     31.184 km      1.4 cm    72323     3.9%    97.4%    1, 3, 5,...
 broa-umbc     33.271 km      1.6 cm    69211     6.1%    98.6%    1, 3, 5,...
 baco-godz     46.042 km      1.3 cm    55070     1.9%    99.3%    2, 4, 6
 wal1-godz     47.936 km      1.9 cm    44672    19.7%    96.7%    2, 4, 6
 wdc5-umbc     48.326 km      1.2 cm    90974     0.2%    98.8%    1, 3, 5,...
 ros1-umbc     54.375 km      1.6 cm    40255    16.1%    96.8%    1, 3, 5, 8
 wal1-umbc     75.651 km      2.0 cm    58552    18.8%    95.7%    1, 3, 5,...
 cov1-godz     78.794 km      1.2 cm    54185     1.6%    99.2%    2, 4, 6
 lex1-godz     90.184 km      1.6 cm    44150    19.0%    93.5%    2, 4, 6
 dene-umbc     95.500 km      1.4 cm    91251     0.9%    96.5%    1, 3, 5,...
 cov1-umbc     99.817 km      1.3 cm    71252     1.5%   100.0%    1, 3, 5,...
 lex1-umbc    112.511 km      1.7 cm    53166    18.7%    94.1%    3, 5, 7, 8
 loyo-godz    117.013 km      1.3 cm    54122     1.8%    99.5%    2, 4, 6
 dene-godz    118.388 km      1.4 cm    54263     1.1%    98.5%    2, 4, 6
 loyo-umbc    144.931 km      1.5 cm    90097     1.3%    99.4%    1, 3, 5,...
 stkr-godz    457.384 km      1.2 cm    52981     1.2%    93.4%    2, 4, 6
 stkr-umbc    465.378 km      1.4 cm    89159     0.9%    96.1%    1, 3, 5,...

 MARK  ESTIMATED - A PRIORI COORDINATE SHIFTS
-------------------------------------------------------------------------------
 arno  N:    0.000 m (0.000 m) E:   -0.001 m (0.000 m) H:    0.003 m (0.001 m)
 baco  N:    0.000 m (0.000 m) E:    0.000 m (0.000 m) H:    0.000 m (0.000 m)
 broa  N:   -0.002 m (0.000 m) E:   -0.001 m (0.000 m) H:   -0.006 m (0.001 m)
 cov1  N:   -0.003 m (0.000 m) E:   -0.002 m (0.000 m) H:   -0.001 m (0.001 m)
 crof  N:   -0.002 m (0.000 m) E:    0.002 m (0.000 m) H:    0.005 m (0.001 m)
 dene  N:   -0.003 m (0.000 m) E:   -0.001 m (0.000 m) H:   -0.001 m (0.000 m)
 gode  N:   -0.001 m (0.000 m) E:   -0.001 m (0.000 m) H:    0.004 m (0.000 m)
 godz  N:    0.000 m (0.000 m) E:    0.000 m (0.000 m) H:    0.002 m (0.000 m)
 lex1  N:    0.000 m (0.000 m) E:    0.002 m (0.000 m) H:   -0.007 m (0.001 m)
 loyo  N:   -0.002 m (0.000 m) E:    0.000 m (0.000 m) H:   -0.002 m (0.000 m)
 ros1  N:   -0.006 m (0.000 m) E:    0.001 m (0.000 m) H:    0.037 m (0.001 m)
 stkr  N:    0.002 m (0.000 m) E:   -0.005 m (0.000 m) H:    0.000 m (0.001 m)
 umbc  N:    0.000 m (0.000 m) E:   -0.001 m (0.000 m) H:    0.003 m (0.000 m)
 wal1  N:   -0.004 m (0.000 m) E:    0.000 m (0.000 m) H:   -0.002 m (0.001 m)
 wdc5  N:    0.000 m (0.000 m) E:   -0.001 m (0.000 m) H:   -0.003 m (0.000 m)

++++++++++++++++++++++++++++++++++++++++++++++++++++++++++++++++++++++++++++++++
UNCONSTRAINED MARKS
++++++++++++++++++++++++++++++++++++++++++++++++++++++++++++++++++++++++++++++++

MARK:      arno (arno    1)

REF FRAME:        NAD_83(2011) @ 2010.0000              ITRF2014 @ 2020.7665
X:                1158910.178 m    0.000 m          1158909.261 m    0.000 m
Y:               -4823629.188 m    0.000 m         -4823627.744 m    0.000 m
Z:                3995327.612 m    0.000 m          3995327.560 m    0.000 m
LAT:           39 02 05.52428      0.000 m       39 02 05.55603      0.000 m
E LON:        283 30 34.73965      0.000 m      283 30 34.71660      0.000 m
W LON:         76 29 25.26035      0.000 m       76 29 25.28340      0.000 m
EL HGT:                4.906 m    0.001 m                3.616 m    0.001 m
ORTHO HGT:            38.161 m    0.015 m  (= EL HGT - -33.255 GEOID18 HGT)

                UTM COORDINATES    STATE PLANE COORDINATES
                 UTM (Zone 18)         SPC (1900 MD)
NORTHING (Y)      4321702.614 m         152000.081 m
EASTING (X)        371008.294 m         444125.189 m
CONVERGENCE       -0.93874167 deg       0.31987500 deg
POINT SCALE        0.99980488           0.99995369
```

Appendix B. Continued.

```
COMBINED FACTOR    0.99980411           0.99995292

US NATIONAL GRID DESIGNATOR: 18SUJ7100821702 (NAD 83)

++++++++++++++++++++++++++++++++++++++++++++++++++++++++++++++++++++++++++++++++++++++

MARK:      broa (broa    1)

REF FRAME:        NAD_83(2011) @ 2010.0000              ITRF2014 @ 2020.7666
X:                 1154021.089 m    0.000 m          1154020.171 m    0.000 m
Y:                -4828609.402 m    0.000 m         -4828607.958 m    0.000 m
Z:                 3990739.543 m    0.000 m          3990739.491 m    0.000 m
LAT:            38 58 54.31409      0.000 m       38 58 54.34579      0.000 m
E LON:         283 26 28.89549      0.000 m      283 26 28.87236      0.000 m
W LON:          76 33 31.10451      0.000 m       76 33 31.12764      0.000 m
EL HGT:                -4.918 m    0.001 m               -6.208 m    0.001 m
ORTHO HGT:             28.267 m    0.015 m  (= EL HGT - -33.185 GEOID18 HGT)

                UTM COORDINATES    STATE PLANE COORDINATES
                 UTM (Zone 18)         SPC (1900 MD)
NORTHING (Y)      4315907.110 m         146073.155 m
EASTING (X)        364996.449 m         438241.233 m
CONVERGENCE       -0.98064722 deg       0.27701389 deg
POINT SCALE        0.99982443           0.99995155
COMBINED FACTOR    0.99982520           0.99995232

US NATIONAL GRID DESIGNATOR: 18SUJ6499615907 (NAD 83)

++++++++++++++++++++++++++++++++++++++++++++++++++++++++++++++++++++++++++++++++++++++

MARK:      cov1 (cov1    1)

REF FRAME:        NAD_83(2011) @ 2010.0000              ITRF2014 @ 2020.7665
X:                 1175163.269 m    0.000 m          1175162.356 m    0.000 m
Y:                -4866014.481 m    0.000 m         -4866013.028 m    0.000 m
Z:                 3939155.597 m    0.000 m          3939155.541 m    0.000 m
LAT:            38 23 11.16082      0.000 m       38 23 11.19217      0.000 m
E LON:         283 34 37.91857      0.000 m      283 34 37.89604      0.000 m
W LON:          76 25 22.08143      0.000 m       76 25 22.10396      0.000 m
EL HGT:                -0.213 m    0.001 m               -1.523 m    0.001 m
ORTHO HGT:             34.179 m    0.017 m  (= EL HGT - -34.392 GEOID18 HGT)

                UTM COORDINATES    STATE PLANE COORDINATES
                 UTM (Zone 18)         SPC (1900 MD)
NORTHING (Y)      4249650.221 m          80056.595 m
EASTING (X)        375737.320 m         450428.640 m
CONVERGENCE       -0.88361944 deg       0.36226944 deg
POINT SCALE        0.99979016           0.99998609
COMBINED FACTOR    0.99979019           0.99998612

US NATIONAL GRID DESIGNATOR: 18SUH7573749650 (NAD 83)

++++++++++++++++++++++++++++++++++++++++++++++++++++++++++++++++++++++++++++++++++++++

MARK:      crof (crof    1)

REF FRAME:        NAD_83(2011) @ 2010.0000              ITRF2014 @ 2020.7666
X:                 1143680.970 m    0.000 m          1143680.053 m    0.000 m
Y:                -4828541.811 m    0.001 m         -4828540.368 m    0.001 m
Z:                 3993797.479 m    0.000 m          3993797.427 m    0.000 m
LAT:            39 01 01.56283      0.000 m       39 01 01.59449      0.000 m
E LON:         283 19 31.50646      0.000 m      283 19 31.48319      0.000 m
```

Appendix B. Continued.

```
W LON:         76 40 28.49354      0.000 m       76 40 28.51681      0.000 m
EL HGT:                8.352 m    0.001 m               7.064 m    0.001 m
ORTHO HGT:            41.167 m    0.015 m  (= EL HGT - -32.815 GEOID18 HGT)

               UTM COORDINATES    STATE PLANE COORDINATES
                UTM (Zone 18)         SPC (1900 MD)
NORTHING (Y)      4320008.247 m         149954.803 m
EASTING (X)        355025.632 m         428181.656 m
CONVERGENCE       -1.05441944 deg       0.20424444 deg
POINT SCALE        0.99985880           0.99995288
COMBINED FACTOR    0.99985749           0.99995157

US NATIONAL GRID DESIGNATOR: 18SUJ5502520008 (NAD 83)

++++++++++++++++++++++++++++++++++++++++++++++++++++++++++++++++++++++++++++++++++++++

MARK:      lex1 (lex1    1)

REF FRAME:        NAD_83(2011) @ 2010.0000              ITRF2014 @ 2020.7668
X:                1174354.963 m    0.000 m          1174354.050 m    0.000 m
Y:               -4874932.335 m    0.001 m         -4874930.880 m    0.001 m
Z:                3928427.078 m    0.000 m          3928427.021 m    0.000 m
LAT:           38 15 47.65650      0.000 m       38 15 47.68774      0.000 m
E LON:        283 32 39.48254      0.000 m      283 32 39.46005      0.000 m
W LON:         76 27 20.51746      0.000 m       76 27 20.53995      0.000 m
EL HGT:               -0.774 m    0.001 m               -2.087 m    0.001 m
ORTHO HGT:            33.730 m    0.017 m  (= EL HGT - -34.504 GEOID18 HGT)

               UTM COORDINATES    STATE PLANE COORDINATES
                UTM (Zone 18)         SPC (1900 MD)
NORTHING (Y)      4236024.451 m          66364.197 m
EASTING (X)        372648.468 m         447635.907 m
CONVERGENCE       -0.90160000 deg       0.34162222 deg
POINT SCALE        0.99979974           1.00000660
COMBINED FACTOR    0.99979986           1.00000672

US NATIONAL GRID DESIGNATOR: 18SUH7264836024 (NAD 83)

++++++++++++++++++++++++++++++++++++++++++++++++++++++++++++++++++++++++++++++++++++++

MARK:      ros1 (ros1    1)

REF FRAME:        NAD_83(2011) @ 2010.0000              ITRF2014 @ 2020.7657
X:                1135286.273 m    0.000 m          1135285.357 m    0.000 m
Y:               -4847925.437 m    0.001 m         -4847923.990 m    0.001 m
Z:                3972839.228 m    0.001 m          3972839.173 m    0.001 m
LAT:           38 46 27.61178      0.000 m       38 46 27.64324      0.000 m
E LON:        283 10 48.03313      0.000 m      283 10 48.00985      0.000 m
W LON:         76 49 11.96687      0.000 m       76 49 11.99015      0.000 m
EL HGT:               35.107 m    0.001 m               33.812 m    0.001 m
ORTHO HGT:            67.895 m    0.016 m  (= EL HGT - -32.788 GEOID18 HGT)

               UTM COORDINATES    STATE PLANE COORDINATES
                UTM (Zone 18)         SPC (1900 MD)
NORTHING (Y)      4293307.800 m         122971.225 m
EASTING (X)        341898.641 m         415642.190 m
CONVERGENCE       -1.14001389 deg       0.11298056 deg
POINT SCALE        0.99990781           0.99995141
COMBINED FACTOR    0.99990230           0.99994590

US NATIONAL GRID DESIGNATOR: 18SUH4189893307 (NAD 83)
```

Appendix B. Continued.

++

MARK: stkr (stkr a 3)

REF FRAME:	NAD_83(2011) @ 2010.0000			ITRF2014 @ 2020.7664	
X:	678451.038 m	0.000 m		678450.121 m	0.000 m
Y:	-4893799.717 m	0.000 m		-4893798.286 m	0.000 m
Z:	4020496.783 m	0.000 m		4020496.701 m	0.000 m
LAT:	39 19 33.82500	0.000 m		39 19 33.85467	0.000 m
E LON:	277 53 34.37006	0.000 m		277 53 34.34036	0.000 m
W LON:	82 06 25.62994	0.000 m		82 06 25.65964	0.000 m
EL HGT:	178.035 m	0.001 m		176.790 m	0.001 m
ORTHO HGT:	212.221 m	0.018 m	(= EL HGT - -34.186 GEOID18 HGT)		

	UTM COORDINATES (Zone 17)	STATE PLANE COORDINATES SPC (3402 OH S)
NORTHING (Y)	4353545.422 m	147284.043 m
EASTING (X)	404572.963 m	633874.813 m
CONVERGENCE	-0.70166944 deg	0.24929167 deg
POINT SCALE	0.99971212	0.99993642
COMBINED FACTOR	0.99968420	0.99990849

US NATIONAL GRID DESIGNATOR: 17SMD0457253545 (NAD 83)

++

MARK: wal1 (wal1 1)

REF FRAME:	NAD_83(2011) @ 2010.0000			ITRF2014 @ 2020.7666	
X:	1127888.801 m	0.000 m		1127887.887 m	0.000 m
Y:	-4862133.250 m	0.001 m		-4862131.802 m	0.001 m
Z:	3957648.548 m	0.000 m		3957648.492 m	0.000 m
LAT:	38 35 56.63652	0.000 m		38 35 56.66781	0.000 m
E LON:	283 03 36.50707	0.000 m		283 03 36.48378	0.000 m
W LON:	76 56 23.49293	0.000 m		76 56 23.51622	0.000 m
EL HGT:	30.059 m	0.001 m		28.760 m	0.001 m
ORTHO HGT:	62.969 m	0.016 m	(= EL HGT - -32.910 GEOID18 HGT)		

	UTM COORDINATES (Zone 18)	STATE PLANE COORDINATES SPC (1900 MD)
NORTHING (Y)	4274070.441 m	103501.654 m
EASTING (X)	331073.117 m	405238.857 m
CONVERGENCE	-1.21050000 deg	0.03774722 deg
POINT SCALE	0.99995142	0.99996145
COMBINED FACTOR	0.99994670	0.99995673

US NATIONAL GRID DESIGNATOR: 18SUH3107374070 (NAD 83)

++
CONSTRAINED MARKS
++

MARK: baco (baco a 2)

CONSTRAIN: 3-D NORMAL

N39:23:58.03744 W076:36:24.44316	128.305m		NAD_83(2011) @ 2010.0000	
0.12cm	0.11cm	0.12cm	NEU SIGMAS	
SHIFTS N:	0.000 m (0.000 m)	E: 0.000 m (0.000 m)	H:	0.000 m (0.000 m)

REF FRAME:	NAD_83(2011) @ 2010.0000			ITRF2014 @ 2020.7663	
X:	1143199.185 m	0.000 m		1143198.264 m	0.000 m
Y:	-4801171.607 m	0.000 m		-4801170.167 m	0.000 m

Appendix B. Continued.

```
Z:                4026765.138 m    0.000 m          4026765.090 m    0.000 m
LAT:           39 23 58.03746      0.000 m       39 23 58.06947      0.000 m
E LON:        283 23 35.55685      0.000 m      283 23 35.53336      0.000 m
W LON:         76 36 24.44315      0.000 m       76 36 24.46664      0.000 m
EL HGT:              128.304 m    0.000 m              127.026 m    0.000 m
ORTHO HGT:           160.872 m    0.015 m  (= EL HGT - -32.568 GEOID18 HGT)

               UTM COORDINATES    STATE PLANE COORDINATES
                UTM (Zone 18)         SPC (1900 MD)
NORTHING (Y)     4362337.559 m         192424.921 m
EASTING (X)       361647.403 m         433869.643 m
CONVERGENCE      -1.02002778 deg       0.24679167 deg
POINT SCALE       0.99983568           0.99999155
COMBINED FACTOR   0.99981555           0.99997142

US NATIONAL GRID DESIGNATOR: 18SUJ6164762337 (NAD 83)

++++++++++++++++++++++++++++++++++++++++++++++++++++++++++++++++++++++++++++++++++++++

MARK:      dene (dene a  3)
CONSTRAIN: 3-D NORMAL
     N39:40:36.24965 W075:44:34.82897    6.545m        NAD_83(2011) @ 2010.0000
           0.12cm          0.10cm     0.13cm        NEU SIGMAS
SHIFTS N:   -0.003 m (0.000 m) E:   -0.001 m (0.000 m) H:   -0.001 m (0.000 m)

REF FRAME:        NAD_83(2011) @ 2010.0000             ITRF2014 @ 2020.7664
X:                1210598.678 m    0.000 m          1210597.753 m    0.000 m
Y:               -4764306.699 m    0.000 m         -4764305.251 m    0.000 m
Z:                4050429.564 m    0.000 m          4050429.518 m    0.000 m
LAT:           39 40 36.24954      0.000 m       39 40 36.28216      0.000 m
E LON:        284 15 25.17097      0.000 m      284 15 25.14833      0.000 m
W LON:         75 44 34.82903      0.000 m       75 44 34.85167      0.000 m
EL HGT:               6.544 m      0.000 m              5.259 m      0.000 m
ORTHO HGT:           39.546 m      0.015 m  (= EL HGT - -33.002 GEOID18 HGT)

               UTM COORDINATES    STATE PLANE COORDINATES
                UTM (Zone 18)         SPC (0700 DE)
NORTHING (Y)     4392142.875 m         186188.491 m
EASTING (X)       436278.661 m         172001.596 m
CONVERGENCE      -0.47439444 deg      -0.20835556 deg
POINT SCALE       0.99964999           1.00000465
COMBINED FACTOR   0.99964896           1.00000362

US NATIONAL GRID DESIGNATOR: 18SVJ3627892142 (NAD 83)

++++++++++++++++++++++++++++++++++++++++++++++++++++++++++++++++++++++++++++++++++++++

MARK:      gode (gode a  4)
CONSTRAIN: 3-D NORMAL
     N39:01:18.18970 W076:49:36.57471   15.784m        NAD_83(2011) @ 2010.0000
           0.12cm          0.12cm     0.12cm        NEU SIGMAS
SHIFTS N:   -0.001 m (0.000 m) E:   -0.001 m (0.000 m) H:    0.004 m (0.000 m)

REF FRAME:        NAD_83(2011) @ 2010.0000             ITRF2014 @ 2020.7664
X:                1130774.428 m    0.000 m          1130773.507 m    0.000 m
Y:               -4831255.029 m    0.000 m         -4831253.573 m    0.000 m
Z:                3994200.521 m    0.000 m          3994200.462 m    0.000 m
LAT:           39 01 18.18967      0.000 m       39 01 18.22141      0.000 m
E LON:        283 10 23.42525      0.000 m      283 10 23.40177      0.000 m
W LON:         76 49 36.57475      0.000 m       76 49 36.59823      0.000 m
EL HGT:              15.788 m      0.000 m              14.487 m      0.000 m
ORTHO HGT:           48.168 m      0.015 m  (= EL HGT - -32.380 GEOID18 HGT)
```

Appendix B. Continued.

```
                UTM COORDINATES    STATE PLANE COORDINATES
                 UTM (Zone 18)         SPC (1900 MD)
NORTHING (Y)      4320774.469 m         150431.506 m
EASTING (X)        341854.666 m         414996.113 m
CONVERGENCE       -1.15043611 deg       0.10868889 deg
POINT SCALE        0.99990796           0.99995308
COMBINED FACTOR    0.99990548           0.99995060

US NATIONAL GRID DESIGNATOR: 18SUJ4185420774 (NAD 83)

++++++++++++++++++++++++++++++++++++++++++++++++++++++++++++++++++++++++++++++++++++++

MARK:      godz (godz a  4)
CONSTRAIN: 3-D NORMAL
     N39:01:18.18970 W076:49:36.57471   15.784m        NAD_83(2011) @ 2010.0000
             0.13cm           0.07cm     0.13cm        NEU SIGMAS
SHIFTS N:    0.000 m (0.000 m) E:    0.000 m (0.000 m) H:    0.002 m (0.000 m)

REF FRAME:        NAD_83(2011) @ 2010.0000              ITRF2014 @ 2020.7663
X:                1130774.429 m    0.000 m          1130773.507 m    0.000 m
Y:               -4831255.027 m    0.000 m         -4831253.573 m    0.000 m
Z:                3994200.521 m    0.000 m          3994200.462 m    0.000 m
LAT:           39 01 18.18970      0.000 m       39 01 18.22141      0.000 m
E LON:        283 10 23.42531      0.000 m      283 10 23.40178      0.000 m
W LON:         76 49 36.57469      0.000 m       76 49 36.59822      0.000 m
EL HGT:               15.787 m    0.000 m               14.487 m    0.000 m
ORTHO HGT:            48.167 m    0.015 m  (= EL HGT - -32.380 GEOID18 HGT)

                UTM COORDINATES    STATE PLANE COORDINATES
                 UTM (Zone 18)         SPC (1900 MD)
NORTHING (Y)      4320774.470 m         150431.507 m
EASTING (X)        341854.667 m         414996.115 m
CONVERGENCE       -1.15043611 deg       0.10868889 deg
POINT SCALE        0.99990796           0.99995308
COMBINED FACTOR    0.99990548           0.99995060

US NATIONAL GRID DESIGNATOR: 18SUJ4185420774 (NAD 83)

++++++++++++++++++++++++++++++++++++++++++++++++++++++++++++++++++++++++++++++++++++++

MARK:      loyo (loyo a  3)
CONSTRAIN: 3-D NORMAL
     N38:03:00.62625 W077:20:51.17400   43.177m        NAD_83(2011) @ 2010.0000
             0.12cm           0.10cm     0.12cm        NEU SIGMAS
SHIFTS N:   -0.002 m (0.000 m) E:    0.000 m (0.000 m) H:   -0.002 m (0.000 m)

REF FRAME:        NAD_83(2011) @ 2010.0000              ITRF2014 @ 2020.7664
X:                1101542.004 m    0.000 m          1101541.092 m    0.000 m
Y:               -4906910.940 m    0.000 m         -4906909.477 m    0.000 m
Z:                3909857.631 m    0.000 m          3909857.564 m    0.000 m
LAT:           38 03 00.62617      0.000 m       38 03 00.65698      0.000 m
E LON:        282 39 08.82596      0.000 m      282 39 08.80261      0.000 m
W LON:         77 20 51.17404      0.000 m       77 20 51.19739      0.000 m
EL HGT:               43.175 m    0.000 m               41.853 m    0.000 m
ORTHO HGT:            75.859 m    0.021 m  (= EL HGT - -32.684 GEOID18 HGT)

                UTM COORDINATES    STATE PLANE COORDINATES
                 UTM (Zone 18)         SPC (4501 VA N)
NORTHING (Y)      4213983.643 m        2043203.426 m
EASTING (X)        294018.051 m        3601150.708 m
CONVERGENCE       -1.44742222 deg       0.71926667 deg
```

Appendix B. Continued.

```
POINT SCALE        1.00012258           0.99999707
COMBINED FACTOR    1.00011580           0.99999030

US NATIONAL GRID DESIGNATOR: 18STH9401813983 (NAD 83)

++++++++++++++++++++++++++++++++++++++++++++++++++++++++++++++++++++++++++++++++

MARK:      umbc (umbc a  3)
CONSTRAIN: 3-D NORMAL
     N39:15:24.36082 W076:42:41.46870   65.940m        NAD_83(2011) @ 2010.0000
            0.13cm           0.08cm     0.13cm        NEU SIGMAS
SHIFTS N:    0.000 m (0.000 m) E:   -0.001 m (0.000 m) H:    0.003 m (0.000 m)

REF FRAME:        NAD_83(2011) @ 2010.0000             ITRF2014 @ 2020.7665
X:                1136717.966 m    0.000 m          1136717.045 m    0.000 m
Y:               -4812977.290 m    0.000 m         -4812975.842 m    0.000 m
Z:                4014471.592 m    0.000 m          4014471.537 m    0.000 m
LAT:           39 15 24.36081      0.000 m       39 15 24.39270      0.000 m
E LON:        283 17 18.53124      0.000 m      283 17 18.50773      0.000 m
W LON:         76 42 41.46876      0.000 m       76 42 41.49227      0.000 m
EL HGT:               65.942 m    0.000 m              64.652 m    0.000 m
ORTHO HGT:            98.407 m    0.015 m  (= EL HGT - -32.465 GEOID18 HGT)

               UTM COORDINATES    STATE PLANE COORDINATES
                UTM (Zone 18)         SPC (1900 MD)
NORTHING (Y)      4346666.826 m         176550.149 m
EASTING (X)        352329.277 m         424898.749 m
CONVERGENCE       -1.08323889 deg       0.18106111 deg
POINT SCALE        0.99986850           0.99997190
COMBINED FACTOR    0.99985816           0.99996155

US NATIONAL GRID DESIGNATOR: 18SUJ5232946666 (NAD 83)

++++++++++++++++++++++++++++++++++++++++++++++++++++++++++++++++++++++++++++++++

MARK:      wdc5 (wdc5 a  1)
CONSTRAIN: 3-D NORMAL
     N38:55:14.00162 W077:03:58.72342   60.266m        NAD_83(2011) @ 2010.0000
            0.12cm           0.12cm     0.12cm        NEU SIGMAS
SHIFTS N:    0.000 m (0.000 m) E:   -0.001 m (0.000 m) H:   -0.003 m (0.000 m)

REF FRAME:        NAD_83(2011) @ 2010.0000             ITRF2014 @ 2020.7664
X:                1112159.531 m    0.000 m          1112158.614 m    0.000 m
Y:               -4842857.057 m    0.000 m         -4842855.613 m    0.000 m
Z:                3985497.034 m    0.000 m          3985496.980 m    0.000 m
LAT:           38 55 14.00163      0.000 m       38 55 14.03311      0.000 m
E LON:        282 56 01.27657      0.000 m      282 56 01.25287      0.000 m
W LON:         77 03 58.72343      0.000 m       77 03 58.74713      0.000 m
EL HGT:               60.262 m    0.000 m              58.973 m    0.000 m
ORTHO HGT:            92.253 m    0.014 m  (= EL HGT - -31.991 GEOID18 HGT)

               UTM COORDINATES    STATE PLANE COORDINATES
                UTM (Zone 18)         SPC (1900 MD)
NORTHING (Y)      4309990.456 m         139189.276 m
EASTING (X)        320866.234 m         394249.493 m
CONVERGENCE       -1.29848889 deg      -0.04161944 deg
POINT SCALE        0.99999515           0.99995015
COMBINED FACTOR    0.99998570           0.99994070

US NATIONAL GRID DESIGNATOR: 18SUJ2086609990 (NAD 83)
```

Appendix C. CORS data, horizontal movement of CORS stations.

CORS	HORIZONTAL VELOCITY (mm/yr.)	DIRECTIONALITY (Degrees West of North)
ANP5	14.94	74.67
GODE	15.19	74.54
HNPT	14.56	73.32
RED5	15.11	73.51
SOL1	15.2	73.52
USNA	15.52	78.18
USN3	15.47	74.28

Appendix D. CORS used in regional land subsidence map.

4CID	State	Longitude, Latitude (ITRF14)	VLM (mm/yr)
ALLG	MD	-78.730700753, 39.653866342	1.2
ANP1	MD	-76.609200000, 39.010300000	1.8
ANP5	MD	-76.60924683, 39.01028683	2.6
ATLC	NJ	-74.418333333, 39.356666667	2.2
BACO	MD	-76.60679, 39.39945	0.2
BALT	MD	-76.58, 39.266666667	1.3
BLKV	VA	-80.414526361, 37.206018042	1.6
CAMB	MD	-76.061666667, 38.571666667	1.9
CHES	PA	-75.600324544, 39.951653083	0.7
CHL1	DE	-75.087685749, 38.776787585	2.0
CHR1	VA	-76.006370192, 36.927080581	1.6
COLB	VA	-76.96, 38.251666667	3.1
CORB	VA	-77.37349423, 38.202182028	1.2
CSPK	MD	-75.81, 39.526666667	1.3
DEDS	DE	-75.377437114, 38.664533942	2.4
DEMI	DE	-75.202869367, 38.610279333	1.9
DENE	DE	-75.67635, 39.67674	1.0
DNRC	DE	-75.52360000, 39.160090000	2.5
DRV1/5	VA	-76.556643894, 36.958656928	3.8
DRV6	VA	-76.556450438, 36.958495165	3.0
GAIT	MD	-77.22098, 39.13399	0.2
GLPT	VA	-76.499455635, 37.248540237	2.4
GODE	MD	-76.82679749, 39.02170181	1.3
GTS1	PA	-76.82635, 40.25217	0.4
HAG6	MD	-77.7141000, 39.553480	1.4
HNPT	MD	-76.1309967, 38.58800125	3.3
HTCC	MD	-77.667394514, 39.632231131	1.0
KIPT	VA	-75.988333333, 37.165	1.9
LANC	PA	-76.304246067, 40.039401333	-0.9
LEWS	VA	-76.465, 37.995	2.4
LOY2	VA	-76.23780095, 36.764016628	1.7
LOY4	VA	-77.563834158, 39.112868775	1.5
LOY5	VA	-77.436264742, 38.886645961	0.2
LOY8	VA	-77.45263, 38.28298	1.7
LOY9	VA	-77.266495703, 39.177317342	0.1
LOYA	VA	-78.889387086, 38.426091508	1.0
LOYB	VA	-77.183976483, 38.728347689	2.4
LOYC	VA	-78.200729872, 39.120159981	0.4
LOYF	VA	-76.522194, 38.974472	2.0
LOYH	VA	-79.324498583, 37.302716167	2.3
LOYJ	VA	-78.010045744, 38.472478503	1.1
LOYK	VA	-76.790632286, 39.131080175	0.7
LOYM	MD	-76.63277505, 38.31059685	2.5
LOYO	VA	-77.347553064, 38.050182125	1.1
LOYQ	MD	-77.714198936, 39.634062175	2.5

Appendix D. Continued.

4CID	State	Longitude, Latitude (ITRF14)	VLM (mm/yr)
LOYR	MD	-75.987503125, 39.569099383	1.5
LOYX	VA	-76.695509861, 37.276405444	2.3
LOYY	VA	-78.499156164, 38.888493625	0.5
LOYZ	VA	-76.573562331, 36.863596667	0.7
LS03	VA	-75.959540192, 36.788740369	2.7
LS04	VA	-79.957497086, 37.363102017	1.3
LS06	VA	-78.292723214, 36.6132118	0.1
LWX1	VA	-77.488603315, 38.972683906	2.1
NJBR	NJ	-75.207064108, 39.423408681	2.0
NJCM	NJ	-74.802899717, 39.100674422	2.4
NJGC	NJ	-75.119795914, 39.781339678	2.1
NJGT	NJ	-74.53081809, 39.4745232	1.3
NRL1	DC	-77.024403, 38.820747	1.2
OCNI	MD	-75.091666667, 38.328333333	2.7
P817	PA	-78.511168678, 40.145580467	0.9
PACO	PA	-75.862775831, 39.980064433	0.1
PAFC	PA	-77.669773869, 39.947067775	0.6
PAFM	PA	-77.978787894, 39.962484069	0.9
PAFU	PA	-79.697369703, 39.926588586	1.4
PAGW	PA	-80.160110533, 39.898930092	1.5
PAPH	PA	-75.176334283, 40.013161278	0.8
RED1	DE	-75.569983181, 39.561452053	2.8
RIC1	VA	-77.429664408, 37.537905036	1.0
SEWP	VA	-76.33, 36.946666667	2.6
SOL1	MD	-76.45389431, 38.31887652	2.8
UMBC	MD	-76.71152, 39.25677	0.9
USN3	MD	-77.06627389, 38.92056472	0.6
USNA	DC	-76.48, 38.983	-0.3
USNO	DC	-77.06622465, 38.91896265	1.1
UVFM	VA	-78.69368, 37.87875	0.9
VA01	VA	-78.014752, 38.020555	1.0
VAGP	VA	-76.49937, 37.24862	3.9
VARI	VA	-77.40239, 37.28998	1.1
VAST	VA	-79.047562225, 38.160497814	0.9
VAWI	VA	-75.4711, 37.93431	3.7
VIMS	VA	-75.68700198, 37.60835358	2.1
WVBU	WV	-78.913501828, 39.338014317	1.4
WVCV	WV	-79.456952639, 39.015307106	1.8
WVMF	WV	-78.932504872, 39.075659428	2.8
WVMO	WV	-79.969920306, 39.645889867	1.6
WVTA	WV	-79.514714783, 39.437964914	-0.6
YORK	PA	-76.740154031, 39.987029883	0.9
ZDC1	DC	-77.54274, 39.1016	1.2

A message to Maryland's citizens

The Maryland Department of Natural Resources (DNR) seeks to balance the preservation and enhancement of the living and physical resources of the state with prudent extraction and utilization policies that benefit the citizens of Maryland. This publication provides information that will increase your understanding of how DNR strives to reach that goal through the earth science assessments conducted by the Maryland Geological Survey.

MARYLAND DEPARTMENT OF NATURAL RESOURCES
Resource Assessment Service
Tawes State Office Building
580 Taylor Avenue
Annapolis, Maryland 21401
Toll free in Maryland: 877-620-8DNR
Out of State call: 410-260-8021
TTY users: Call via the Maryland Relay
Internet Address: dnr.Maryland.gov

MARYLAND GEOLOGICAL SURVEY
2300 St. Paul Street
Baltimore, Maryland 21218
Telephone Contact Information: 410-554-5500
Internet Address: mgs.md.gov

DNR Publication No. 12-082021-286